Gold(I) and Silver(I) Complexes with 2-Anilino-pyridine Based Heterocycles as Multitarget Drugs Against Colon Cancer

*Inés Mármol,[a,b] Sara Montanel-Perez,[a] José Carlos Royo,[b] M. Concepción Gimeno,[*a] M. Dolores Villacampa,[a] M. Jesús Rodríguez-Yoldi, [*b] and Elena Cerrada,[*a]*

[a]Departamento de Química Inorgánica, Instituto de Síntesis Química y Catálisis Homogénea-ISQCH, Universidad de Zaragoza-C.S.I.C., 50009 Zaragoza, Spain. E-mail: ecerrada@unizar.es; gimeno@unizar.es

[b]Departamento de Farmacología y Fisiología. Unidad de Fisiología, Universidad de Zaragoza, 50013, Zaragoza, Spain, CIBERobn, IIS Aragón, IA2. E-mail: mjrodyol@unizar.es

KEYWORDS

Thioredoxin reductase, Proteasome, Gold(I), Silver(I), Colon cancer

Abstract

A series of gold(I) and silver(I) derivatives with N- or S-donor ligands derived from 2-anilino-pyridine has been synthesised and characterised. The mononuclear structure of [Au(L1)(PPh_3)](TfO) (**1a**) and [Au(L2)(PPh_3)](TfO) (**1b**) was confirmed by X-Ray diffraction studies, as well as the dinuclear structure in the case of [Ag(TfO)(L1)]$_2$ (**4a**). Most of the complexes are cytotoxic against a model of colorectal adenocarcinoma (Caco-2 cell line) and breast adenocarcinoma cancer cell lines (MCF-7). [Au(L1)(PPh_3)](TfO) (**1a**) was able to induce caspases 8 and 3 activation, loss of mitochondrial membrane potential and ROS-dependent cell death on Caco-2 cells upon 24h incubation. In addition, the gold complex **1a** produced a significant inhibition of the redox enzyme thioredoxin reductase as well as 20S proteasome. However, the silver(I) analogue [Ag(TfO)(L1)(PPh_3)] (**2a**) induced cell death independent of inhibition of thioredoxin reductase and 20S proteasome, triggered ROS-independent apoptosis mediated by caspase 8 and 3 activation and loss of mitochondrial membrane potential, which points to different mechanism of action for both derivatives, dependent on the metal center.

1. Introduction

The use of platinum-based anticancer drugs in chemotherapy is accompanied with the presence of side-effects such as gastrointestinal and hematological toxicity in addition to drug-resistance phenomena.[1-2] In order to circumvent these drawbacks new metallodrugs have been designed based in non-platinum metals, such as ruthenium or gold.

Gold complexes interact with cellular proteins[3-5] instead of DNA, the main target of the platinum-based complexes, which suppose an important advantage in order to overcome the limitations found in platinum derivatives. Consequently, gold compounds are an interesting alternative to platinum-based drugs. Thus, a huge amount of gold derivatives, mainly gold(I) complexes, has been tested against different types of cancer cells.[6-14] In addition to gold, other metals such as silver are emerging as potential anticancer agents.[15-23]

Silver complexes have been used as antimicrobial agents for many years[24-27] mainly in the form of inorganic salts or complexes, such as silver nitrate[28] and silver sulfadiazine. The latter is a sulfonamide based derivative introduced in 1968[29] and is used as one of the most effective topical burn-treatment,[30] thanks to its antibacterial properties.[31] Although silver is not an endogenous element, its toxicity in humans seems to be quite low. The body can tolerate the presence of silver in low doses without any toxic effects;[32] consequently this low toxicity constitutes one of the greatest advantages of silver derivatives over other metallodrugs.

The mechanism of the anticancer activity of the silver derivatives is not well established, however, several possible targets have been identified. Thus, some examples have exerted antiproliferative effects by inhibition of the activity of the redox enzyme thioredoxin reductase (TrxR),[33] by non-covalent interaction with DNA[34] (interactions as $\pi-\pi$ stacking contacts),[35] by topoisomerase I inhibition[36] or by LOX (lipoxygenase) inhibition activity.[34] In general, silver complexes induce cell death *via* apoptosis and depolarisation of the mitochondrial membrane potential.[37]

Although the mechanism of action of silver derivatives has not been fully clarified, it involves the release of the silver ion inside the cell that disrupts its function.[38] Consequently the choice of the ligands that can strongly coordinate the metallic center and facilitate the slow release of Ag^+ is essential. With this idea, a significant amount of silver complexes with a great variety of ligands has been designed for potential

pharmaceutical usage.[16, 18-19, 21] Thus, silver N-heterocyclic carbene (NHC) complexes [15, 17, 22-24,39] constitute the group with the largest number of examples of Ag(I) compounds with biological properties, mainly due to their strong coordination to the metallic center and their increased stability. Apart from Ag-NHC derivatives, silver coordination compounds with a high number of different ligands (carboxylic acids ligands;[40] phosphines;[41-42] aminoacids ligands;[43] N-donor ligands;[44-45] S-donor ligands[46] and mixed ligands, such as N,O-,[47-48] N,S-,[49] P,O-donor ligands[50]) have been recently described as potential anticancer silver-based complexes.

With this background, we describe here the synthesis of new heterocyclic N- and N,S-donor ligands derived from 2-anilinopyridine containing also thiophene or pyridine moieties. The choice of the anilino moiety is based on the properties exhibited by heterocyclic systems and molecules based on this unit.[51-52] Furthermore, the easy functionalisation with pyridine of thiophene, the latter a five-membered aromatic sulfur-containing heterocycle encountered in many therapeutically active agents, may confer to these ligands interesting biological properties.[53-54] Additionally, coordination to silver and gold metallic centers may enhance those properties. New mononuclear silver derivatives, their gold analogs and dinuclear Ag(I) complexes have been described and their biological activity evaluated against Caco-2 and MCF-7 cancer cells. Redox enzymes thioredoxin reductase and glutathione reductase (GR) as well as 20S proteasome have been investigated as likely targets of selected gold(I) and silver(I) complexes. Moreover, measurement of reactive oxygen species (ROS) and cell death studies have been performed.

2. Results and Discussion

2.1. Synthesis of ligands and complexes.

The reaction of 2-anilinopyridine with 4-chlorocarbonylpyridine or 2-chlorocarbonylthiophene in the presence of NEt_3, in order to neutralise the HCl generated, affords the corresponding ligands **L1** (R = 4-pyridine) and **L2** (R = 2-thiophene) after amide bond formation (Scheme 1).

The addition of both ligands to a freshly prepared solution of [Au(OTf)(PPh_3)] or to a solution of [Ag(OTf)(PPh_3)] leads to the formation of the phosphane gold(I) complexes [AuL(PPh_3)]TfO (L = L1, **1a** and L2, **1b**) and the phosphane silver(I) derivatives [Ag(OTf)L(PPh_3)] (L = L1, **2a** and L2, **2b**, scheme 1)

The asymmetric sulfonyl stretching frequencies characteristic of ionic triflate group[55] are observed in the IR spectra of both gold complexes (**1a-b**), which is corroborated in their $^{19}F\{^{1}H\}$ NMR with a singlet centered at -80 ppm. However, silver derivatives (**2a-b**) exhibit a downfield signal in their $^{19}F\{^{1}H\}$ NMR spectra at around -78 ppm, characteristic of a coordinated triflate ligand and the absence of the band in the region of 1260 cm^{-1}, attributed to ionic TfO in their IR spectra.

A downfield displacement of the pyridine resonances next to the carbonyl moiety is observed in the ^{1}H NMR spectra of complexes **1a** and **2a**, which is in accordance with the coordination of the $AuPPh_3$ moiety through the N atom of that pyridine. Ligand **L2** has replaced such pyridine by a thiophene unit, which signals remain unchanged after gold coordination in complexes **1b** and **2b**. Instead, the resonances of the pyridine molecule of the amine are shifted downfield, due to the coordination of the metallic center through its N atom.

The $^{31}P\{^{1}H\}$ NMR spectra of the gold derivatives display a singlet centered at around 30 ppm, which points to the presence of a unique $AuPPh_3$ fragment. In the case of silver complexes, their $^{31}P\{^{1}H\}$ NMR spectra show a broad signal at room temperature, that split into two doublets at 200 K, due to the coupling of the phosphorus atom with silver isotopomers (^{109}Ag and ^{107}Ag).

The addition of two equivalents of $[Ag(OTf)(PPh_3)]$ to ligands **L1** and **L2** lead to the preparation of the dinuclear phosphane silver(I) derivatives **3a** and **3b** (scheme 1). The NMR data of these complexes are in accordance with the coordination of two $AgPPh_3$ fragments to both pyridine units in **3a** and to the pyridine and thiophene molecules in **3b**. Likewise, the occurrence of two sets of two doublets in the $^{31}P\{^{1}H\}$ NMR spectra at 200 K in **3b** is in agreement with two different phosphorus environment as a consequence of the coordination of the $AgPPh_3$ fragments to the pyridine and thiophene rings through the N and S atom, respectively. However, only two doublets are observed in **3a** pointing to a similar coordination environment since two pyridine rings are coordinated to the $AgPPh_3$ units. In addition, complex **3a**, display two set of doublets with lower intensity, centered at 10.9 ppm, that corresponds to $[Ag(PPh_3)_2]^+$ moiety, which appears in solution along the time.

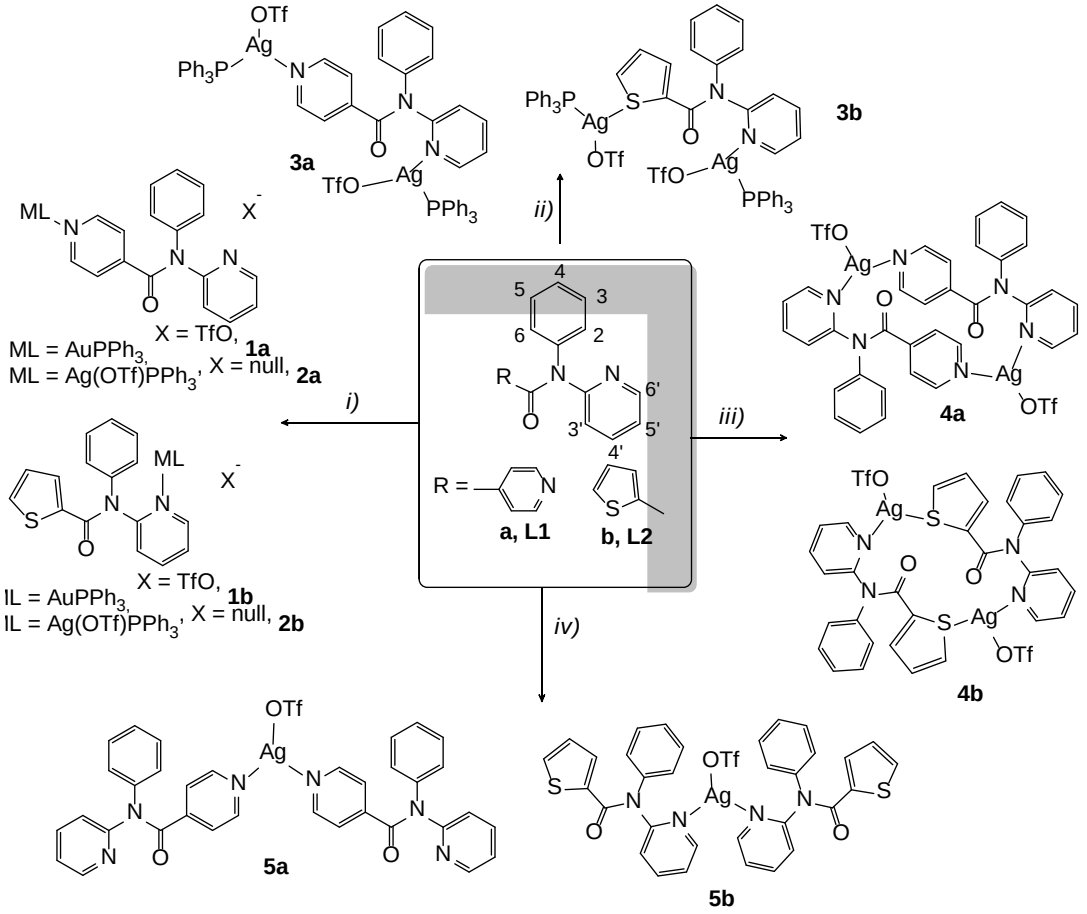

Scheme 1. *i)* [M(OTf)(PPh_3)] (M = Au, **1a-b**; M = Ag, **2a-b**), *ii)* 2 [Ag(OTf)(PPh_3)], *iii)* AgOTf, *iv)* ½ AgOTf

The reaction of AgOTf with **L1** or **L2** in 1:1 and 1:2 molar ratios affords the dinuclear $[Ag_2(OTf)_2L_2]$ (L = L1, **4a**; L2, **4b**) and the mononuclear $[Ag(OTf)L_2]$ (L = L1, **5a**; L2, **5b**) derivatives, respectively (scheme 1). Coordination of the AgOTf fragment to both pyridine molecules in **4a** and to pyridine and thiophene units in **4b** is evidenced by the corresponding NMR downfield displacements and by X-ray analysis in the case of **4a**. On the other hand, ^{1}H NMR of complex **5a** displays solely displacements in the acyl pyridine resonances and **5b** in the pyridine ring of the amine, in accordance with the proposed structure depicted in scheme 1.

All the complexes have been completely characterized by NMR studies, IR spectra, elemental analysis and mass spectra and in the particular cases of **L1**, **L2**, **1a**, **1b** and **4a**, additional X-ray analysis corroborated the proposed structures. The experimental data point to a monodentate coordination of the ligands to the metallic centers of gold or silver

through the N-atom of the ligands, except in the cases of the dinuclear derivatives **3b** and **4b**, where additional coordination to the S atom of ligand **L2** justify the dinuclear structure.

2.2. X-Ray diffraction analyses

Molecular structures of **L1**, **L2** and complexes **1a**, **1b** and **4a** have been confirmed by X-ray crystallographic studies. **L1** and **L2** crystallise in the monoclinic space group $P2_1/c$ with one molecule by asymmetric unit. The molecular structures are shown in Figure S1 (supplementary material) and confirm the nature of the compounds. The bond lengths and angles within then are as expected.

The structure of complex **1a** is shown in Figure 1a. The coordination of the $AuPPh_3$ fragment takes place to the N atom of the acyl pyridine group, with an Au-N and Au-P bond distances of 2.077(5) Å and Au1 P1 2.2371(16) Å, respectively. The geometry around the gold center is slightly distorted from linearity with a P-Au-N angle of 174.46(15)º. The molecules are associated in the lattice due to the presence of intermolecular interactions of the gold center with the oxygen atom of the carbonyl group, Au1···O1 3.003 Å, in addition to hydrogen-bonding interactions with one of the phenyl groups of the PPh_3 ligand, with a distance acceptor-donor O1···H-C36 of 3.278 Å (Figure 1b).

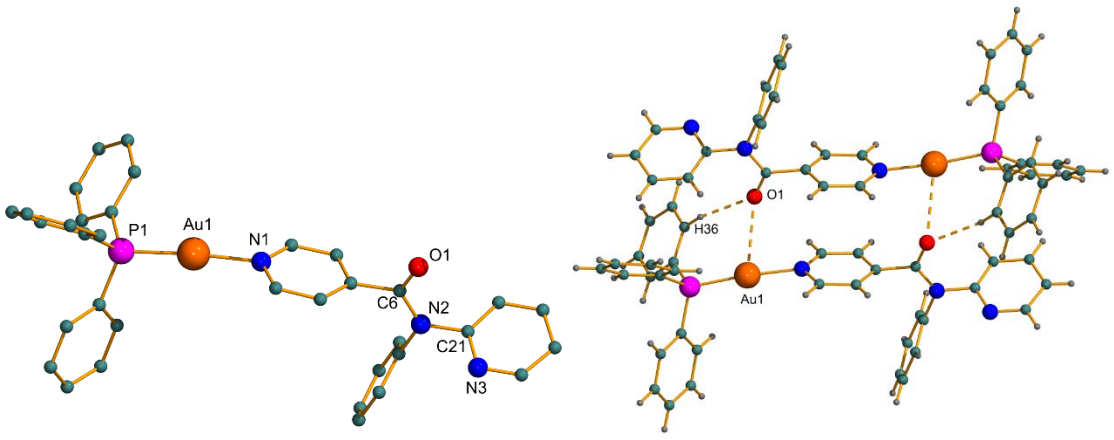

a) b)

Figure 1. a) Molecular structure of the cation of complex **1a**. Hydrogens have been omitted for clarity. b) View of the intramolecular interactions in complex **1a.**

The molecular structure of complex **1b** has also been established by X-ray diffraction and is shown in Figure 2. In contrast to complex **1a** the coordination of the gold atom takes place to the pyridine ring of the 2-anilinopyridine in complex **1b** and not to the sulfur

atom of the thiophene, corroborating the poor nucleophilicity of this moiety. The Au-N and Au-P distances are similar to those in complex **1a**, 2.083(5) Å and 2.2398(16) Å, respectively. The geometry of the gold center is also linear, N-Au-P angle of 175.21(14)º. In this case in probably because the presence of a bulkiest sulfur atom there are not short intermolecular distances in the molecule.

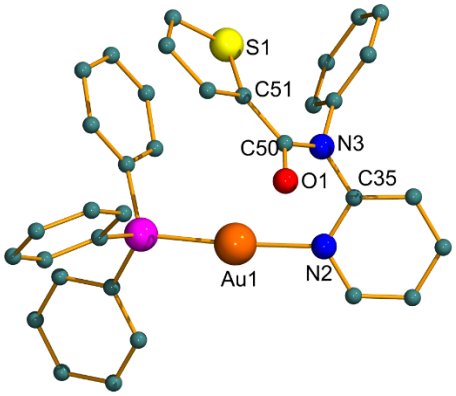

Figure 2. Molecular structure of **1b**, showing the cation. Hydrogens have been omitted for clarity.

The structure of complex **4a** was also measured but the data obtained, although it allows the determination of the molecular structure, is of low quality and consequently not accurate parameters can be obtained. However, the molecule shown in Figure 3 confirms the nature of the compound, presenting an interesting three dimensional polymer, in which there are a dinuclear silver unit with the ligand bonded to the silver through both pyridine groups as bridging ligand. Additionally, the silver atoms bond the oxygen of the carbonyl group and one of the triflare anion forming the 3D network.

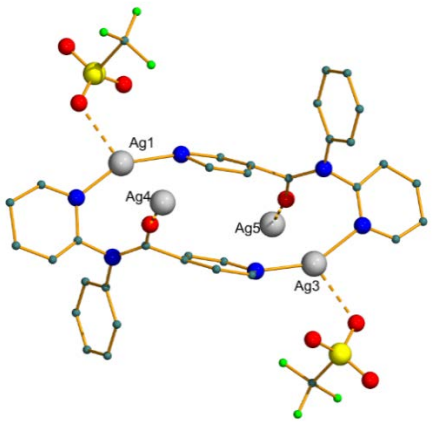

Figure 3. Molecular structure of **4a** showing the basic dinuclear unit and the further contacts with other oxygen atoms.

The stability of the free ligand and complexes was analyzed by UV-vis absorption spectroscopy in PBS solution (pH = 7.4). Solutions suitable for spectrophotometric analysis were prepared by diluting dimethylsulfoxide (DMSO) mother solutions of the complexes with PBS buffer. The resulting solutions were monitored over 24 h at 37 ºC. The spectra of the free ligands and their corresponding complexes (figure S32) show an intense absorption band at *ca.* 210 nm and one lower energy absorption band with low intensity around 260 nm, which could be assigned as $\pi \rightarrow \pi^*$ intraligand transitions. These bands remain without any changes in shape or displacement in the absorbance maximum (none apparent red- or blue shift) in all the new derivatives, in addition to lacking of absorbance at around 500 nm in the case of gold compounds, over 24 h, implying a substantial stability of the chromophore under physiological conditions.

2.3. Biological studies

2.3.1. Antiproliferative effect of gold(I) and silver(I) complexes

The anticancer effect of gold(I) and silver(I) complexes was evaluated on two cell lines: Caco-2, a model of colorectal adenocarcinoma and MCF-7, an estrogen receptor-positive breast carcinoma model. Cell culture was incubated 72h with a range of concentration of each complex and IC_{50} values were obtained. The antiproliferative effect of both ligands was also tested and two reference drugs -cisplatin and auranofin- were included as positive controls. All calculated IC_{50} are shown on Table 1.

Table 1. IC_{50} (μM) values of gold(I) and silver(I) derivatives as well as the free ligands and two reference drugs -cisplatin and auranofin- as positive control on Caco-2, MCF-7 and differentiated Caco-2cells upon 72h incubation. Selectivity Index values are also shown. Results are expressed as mean ± SE of at least three determinations. on after 72h incubation.

Compound	**IC_{50} (μM)**			**Selectivity Index**	
	Caco-2	**MCF-7**	**Differentiated Caco-2 cells**	**Caco-2**	**MCF-7**
L1	>100	17.45 ± 8.16	125.76 ± 13.43	1.26	7.21
[Au(L1)(PPh_3)](TfO) (**1a**)	2.23 ± 0.21	0.46 ± 0.56	39.40 ± 23.39	17.67	85.65
[Ag(TfO)(L1)(PPh_3)] (**2a**)	5.52 ± 1.89	7.22 ± 0.69	9.44 ± 2.12	1.71	1.31
[Ag_2(TfO)$_2$(L1)(PPh_3)$_2$] (**3a**)	0.25 ± 0.10	4.10 ± 0.44	10.88 ± 2.82	43.52	2.65
[Ag(TfO)(L1)]$_2$ (**4a**)	7.50 ± 3.14	>100	48.74 ± 10.01	6.50	-
[Ag(TfO)(L1)$_2$] (**5a**)	10.22 ± 5.02	15.60 ± 1.08	120.51 ± 11.52	11.79	7.73
L2	48.54 ± 13.32	12.48 ± 5.32	124.29 ± 7.50	2.56	9.96

[Au(L2)(PPh_3)](TfO) (**1b**)	3.75 ± 0.41	3.53 ± 0.52	13.53 ± 0.02	3.61	3.83
[Ag(TfO)(L2)(PPh_3)] (**2b**)	7.11 ± 0.92	6.71 ± 0.01	10.23 ± 4.02	1.44	1.52
[Ag_2(TfO)$_2$(L2)(PPh_3)$_2$] (**3b**)	14.41 ± 2.61	7.43 ± 0.49	39.65 ± 19.06	2.75	5.34
[Ag(TfO)(L2)]$_2$ (**4b**)	1.32 ± 0.47	2.65 ± 0.32	55.40 ± 1.43	41.97	20.91
[Ag(TfO)(L2)$_2$] (**5b**)	4.22 ± 2.00	0.90 ± 0.11	80.26 ± 26.90	19.02	89.18
Cisplatin	8.9 ± 0.76[56]	7.6 ± 2.96[57]	-	-	-
Auranofin	1.80 ± 0.10	0.77 ± 0.05	6.21 ± 0.44	3.45	8.06

Most of the evaluated complexes display higher toxicity in comparison to cisplatin in terms of IC_{50}, except complex **4a** which has no antiproliferative effect on MCF-7 cell line. Moreover, IC_{50} of complex **1a** on both cancer models is comparable to those obtained with auranofin, suggesting that **1a** might be a promising antitumor agent.

Although both gold(I) complexes tend to show greater antiproliferative effect than each silver(I) complex analysed, complex **3a** displayed the lowest IC_{50} value, which suggests it might be the most promising agent. However, this compound evolves to an equilibrium of species in DMSO solution, amongst which [Ag(PPh_3)$_2$]TfO was identified. Therefore, the observed anticancer effect might be caused by a mix of molecules instead of a single one and the complex was not considered on further assays.

When comparing the antiproliferative effect of series **1a-5a** and **1b-5b**, results showed on Table 1 suggest minor influence of the ligand **L1** or **L2** on the biological activity of the final metallodrug. However, some exceptions have been observed: complex **1a** displays higher antiproliferative effect than **1b** on MCF-7 cell line; complex **4a** has no effect on MCF-7 cells, whereas **4b** does; finally, **5b** shows greater anticancer effect toward both cell lines than its counterpart **5a**.

The free ligands displayed considerably antiproliferative effect against MCF-7 cells, however, only **L2** showed moderate activity against Caco-2 cells. However, coordination to the metallic center resulted in a significant increase of the antitumor activity, which might suggest that the observed effect depends on both the ligand and the metal. This statement is especially relevant for **1a-5a** series on Caco-2, since the lack of antiproliferative effect of **L1** highlights the key role of gold or silver on the biological activity of the metallodrug. We found no significant differences when comparing IC_{50} values of the free ligands and the new complexes due to the great statistical errors obtained upon IC_{50} calculation of such free ligands. These data suggest that coordination

of the metallic center with the corresponding ligand results in an increase of the antitumor potential compared to the free ligand as well as in an improvement of the reproducibility.

The significant antiproliferative effect displayed by most of the tested complexes as well as the free ligands **L1** and **L2** on MCF-7 cell line was somehow atypical in comparison to previous results obtained by some of us when comparing the effect of selected gold(I) complexes on Caco-2 and MCF-7 cells. In our experience, gold(I) complexes usually show greater anticancer activity on our colorectal adenocarcinoma model rather than on the breast adenocarcinoma one.[58-59] Similar results have been observed by other authors.[60] In a previous work, we found that the alkynyl gold(I) complex [Au(L)PPh_3] (L = 2-(4-bromophenyl)-3-(prop-2-ynyloxy)-4H-chromen-4-one) was able to inhibit cycloocygenase-2 (COX-2) activity; since that isoform is not expressed on MCF-7 cells,[61] the tested complex showed higher antiproliferative effect on other cancer models that actually expressed that enzyme.[58] Given that in our present study we found the opposite effect, we hypothesised that our metallic derivatives might interact with a molecular target found on MCF-7 line but not on Caco-2. As MCF-7 is an estrogen receptor-positive breast adenocarcinoma model, firstly we decided to evaluate the effect of selected complexes on an estrogen receptor-negative MDA-231 cell line to determine their effect on a different subtype of breast adenocarcinoma. As can be observed on Table 2, both gold(I) complexes studied, [Au(L1)(PPh_3)](TfO) (**1a**) and [Au(L2)(PPh_3)](TfO) (**1b**), displayed significant ($p<0.05$) anticancer activity when compared to the free ligands **L1** and **L2** respectively, which suggest that the observed effect is mainly a direct consequence of coordination to the metallic center. Complex **1a** showed a similar behaviour on both breast adenocarcinoma models, thus suggesting that its anticancer effect might be independent of estrogen-receptor expression. On the other hand, the IC_{50} value of **1b** was *ca* 13 times higher on MCF-7 than on MDA-231 cells. Therefore, this complex might be selective for estrogen receptor-positive breast adenocarcinoma cells. It is interesting to highlight that coordination ligand **L2** has no effect on MDA-231 cells, thus it is feasible to assume that the observed effect on this cancer model is due to the presence of the gold atom.

Table 2. IC_{50} (μM) values of gold(I) complexes as well as coordination ligands on MDA-231 cells upon 72h incubation. Results are expressed as mean ± SE of at least three determinations. *p<0.05 *vs* free ligand.

Compound	IC_{50} (μM)
L1	5.69 ± 0.11
[Au(L1)(PPh_3)](TfO) (**1a**)	0.78 ± 0.20*
L2	154.09 ± 0.01
[Au(L2)(PPh_3)](TfO) (**1b**)	0.27 ± 0.05*

In order to evaluate the effect of our complexes on a non-cancerous model, we calculated IC_{50} values after 72h incubation on differentiated Caco-2 cells, which can be used as a gastrointestinal barrier model.[62] Furthermore, we obtained Selectivity Index (SI) using these data and the previous IC_{50} values calculated on cancer models as previously was described by Badisa *et al*.[63] As is shown in Table 1, some of the evaluated complexes displayed higher SI values than the reference drug auranofin, thus suggesting that their clinical use might be safer. In addition, the ligands **L1** and **L2** showed lower SI values than the positive controls and most of the tested complexes. Therefore, although both molecules have previously showed certain antiproliferative effect, they must be discarded as potential anticancer agents due to their likely low selectivity.

Considering all data showed on Table 1, complexes **1a** and **2a** were selected for further assays to determine their likely mechanism of action and kind of cell death triggered upon treatment on Caco-2 cancer cells. Since the unique difference between those complexes was the presence of a gold or silver atom, this would also lead us to perform an in-depth comparison of the anticancer effect based on both metallic centers.

2.3.2. Cell death studies

Caco-2 cells were incubated 48h with the IC_{50} of both complexes **1a** and **2a** and apoptotic populations were analyzed with double annexin V-FITC and propidium iodide staining by flow cytometry. According to Figure 4, neither of the analyzed complexes induced an increase in necrotic population. Instead, upon treatment with complex **1a** a 4.4-up fold on early apoptotic population and a 7-up fold on late apoptotic population were observed. Similarly, the silver complex **2a** triggered a 7.7-up fold on early apoptotic cells along with a 3.6-up fold on late apoptotic cells. Taken together, these results suggest that both

gold(I) and silver(I) complexes are able to induce apoptosis on Caco-2 cells, although the gold-containing derivative seems to trigger cell death faster than the silver(I) counterpart.

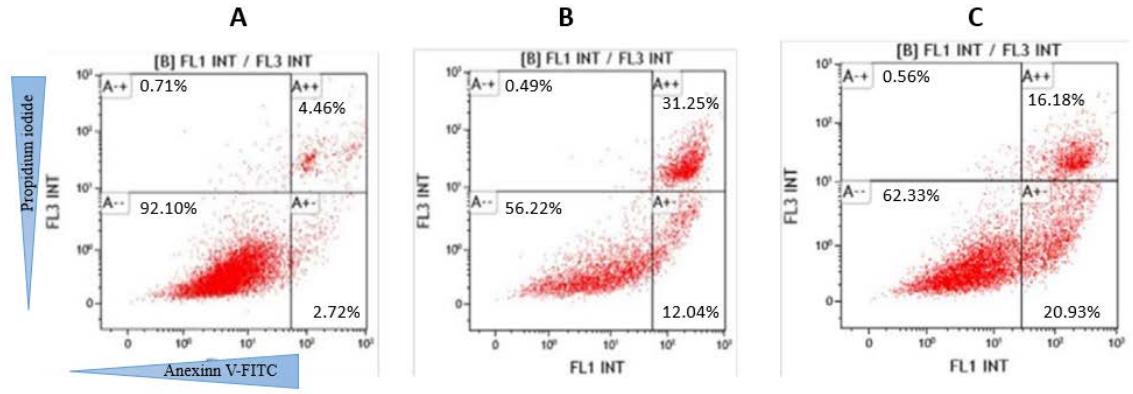

Figure 4. Analysis of the type of cell death induced on undifferentiated Caco-2 cells after 48h incubation with A) DMSO (negative control); B) [Au(L1)(PPh_3)](TfO) (**1a**) (IC_{50}); C) [Ag(TfO)(L1)(PPh_3)] (**2a**) (IC_{50}). Percentages of alive, necrotic, early apoptotic and late apoptotic cells are indicated.

Other apoptotic biomarkers were determined in order to confirm results showed on Figure 4. Since this kind of cell death usually depends on caspases activation,[64-65] we analysed caspase 8 and executioner caspase 3 activation upon 48h of treatment with complexes **1a** and **2a** respectively. We found a significant increase in activation of both caspases (Figure 5A and 5B), which might be in accordance with the increase in apoptotic populations previously observed (Figure 4).

Caspase 8 activation suggests that the tested complexes are able to trigger extrinsic apoptosis. Most of the studies performed in regard to the anticancer activity of gold(I) derivatives have focused on their capacity to induce intrinsic apoptosis; however, some authors have reported that auranofin is also able to trigger cancer cell death *via* extrinsic apoptosis.[66-67] Given that extrinsic apoptosis depends on cell death receptors activation, it remains unclear the mechanism by which auranofin induces this pathway. However, since some authors have noticed that aberrant ROS levels could elicit cell death receptors activation,[68] it has been proposed that the pro-oxidant effect of this metallodrug might be responsible of caspase 8 activation as a consequence. On the other hand, no evidences have been found in regard to further silver(I) complexes able to induce caspase 8 activation to date. To our knowledge, this might be the first report of a silver-containing drug that triggers extrinsic apoptosis on a colorectal cancer model.

Lastly, cell cycle distribution upon 48h of incubation with both complexes **1a** and **2a** was studied. Cell cycle arrest might be indicative of DNA damage and is usually considered

as an apoptotic biomarker as well.[69-70] Treatment with both complexes induced cell cycle arrest on G_1 phase (Figure 5C); gold(I) derivative **1a** triggered a more pronounced arrest than its silver(I) counterpart, which is in accordance with the data previously obtained which suggest that **1a** might be faster than **2a** in regard to its cell death induction capacity.

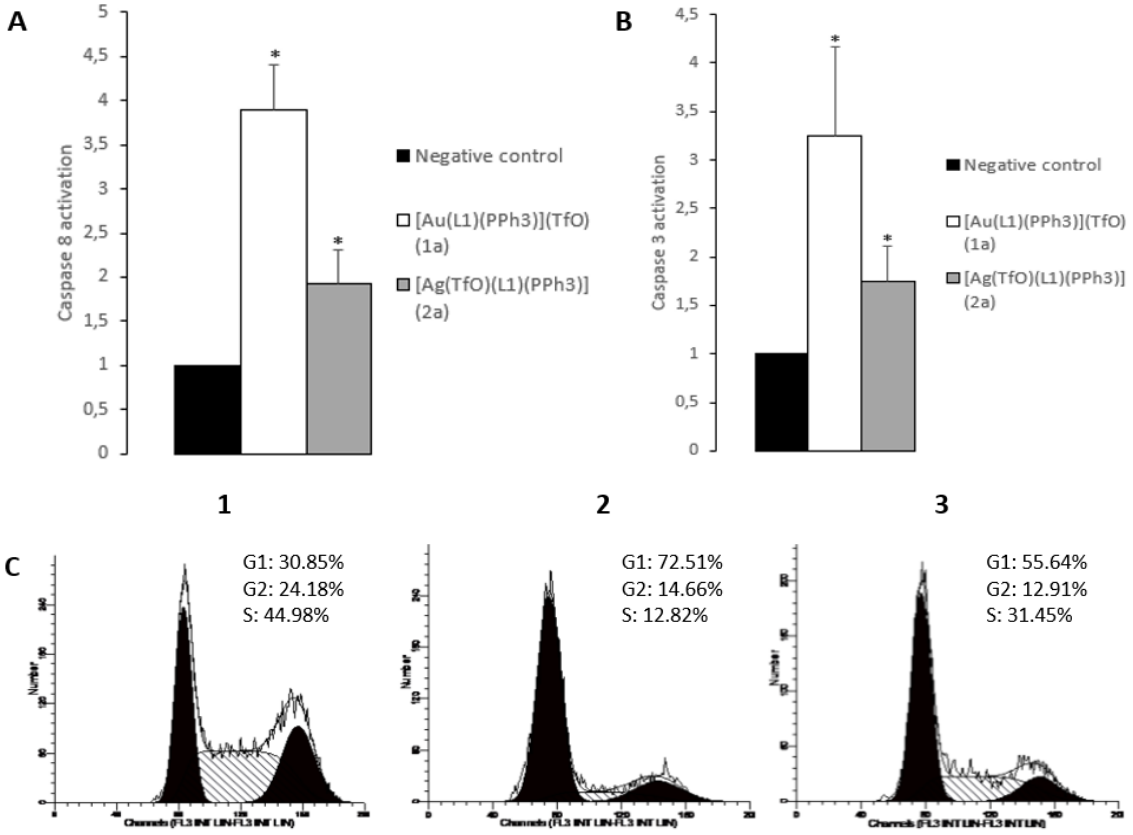

Figure 5. Analysis of apoptosis biomarkers on Caco-2 cells after 48h incubation with complexes **1a** and **2a** (IC_{50}). A) Measurement of caspase 8 activation. *p<0.05 *vs* negative control. B) Measurement of caspase 3 activation. *p<0.05 *vs* negative control. C) Cell cycle analysis. Percentages of cells on each phase are included. Panel 1: negative control (DMSO-treated cells). Panel 2: complex **1a**. Panel 3: complex **2a.**

*2.3.3. Gold(I) complex **1a** and silver(I) complex **2a** disrupts mitochondrial function*

In order to determine the effect of both **1a** and **2a** complexes on mitochondrial function, we analyzed mitochondrial integrity in terms of changes in the mitochondrial membrane potential ($\Delta\psi$). After 48h incubation with IC_{50} value of gold(I) and silver(I) derivatives respectively, we noticed a significant loss on $\Delta\psi$ (Figure 6A). Given that loss of mitochondrial membrane potential might be related to mitochondrial dysfunction and aberrant ROS production, we then measured ROS levels after 24h incubation with both metallodrugs. A significant ($p<0.05$) increase in this parameter was found only upon treatment with the gold complex **1a** (Figure 6B).

Cancer cells have a quite delicate redox balance, and redox homeostasis disruption has been proposed as a promising anticancer approach.[71] In light of results showed on Figure 6B, we evaluated the role of ROS on cell death triggered by complexes **1a** and **2a** using the ROS scavenger N-acetyl-cysteine (NAC). Pre-treatment of Caco-2 cells with NAC resulted in a partial recovery of cell viability decrease induced by complex **1a**, but no modification of cell viability was detected in the cell culture treated with the silver derivative **2a** (Figure 6C). Given that we have previously observed that our silver-containing drug did not disturb redox homeostasis (Figure 6B), this result was not unexpected. Therefore, our results suggest that the silver(I) complex **2a** might trigger ROS-independent apoptosis on Caco-2 cells. Given that pro-oxidant chemotherapeutic agents might damage non-cancer tissues as well, novel drugs able to induce ROS-independent cell death are currently of great interest,[72] thus [Ag(TfO)(L1)(PPh_3)] (**2a**) might be strongly considered as a future anticancer drug.

It is also noticeable that treatment with complex **2a** resulted in a greater loss of $\Delta\psi$ than its gold(I) counterpart and might be related to its mechanism of action. According to data from Eloy *et al*., silver(I) complexes might accumulate on mitochondria and induce mitochondrial dysfunction as a consequence, leading to the release of AIF (Apoptosis-Inducing Factor) and cell death *via* apoptosis. Moreover, authors reported that mitochondrial dysfunction was not accompanied by redox balance disruption,[73] which is in accordance with our current findings.

On the other hand, pre-treatment with NAC did not fully recovered Caco-2 cells incubated with the gold(I) complex **1a**, which suggest that ROS generation might be a part of its mechanism of action, and a ROS-independent cell death mechanism is also involved.

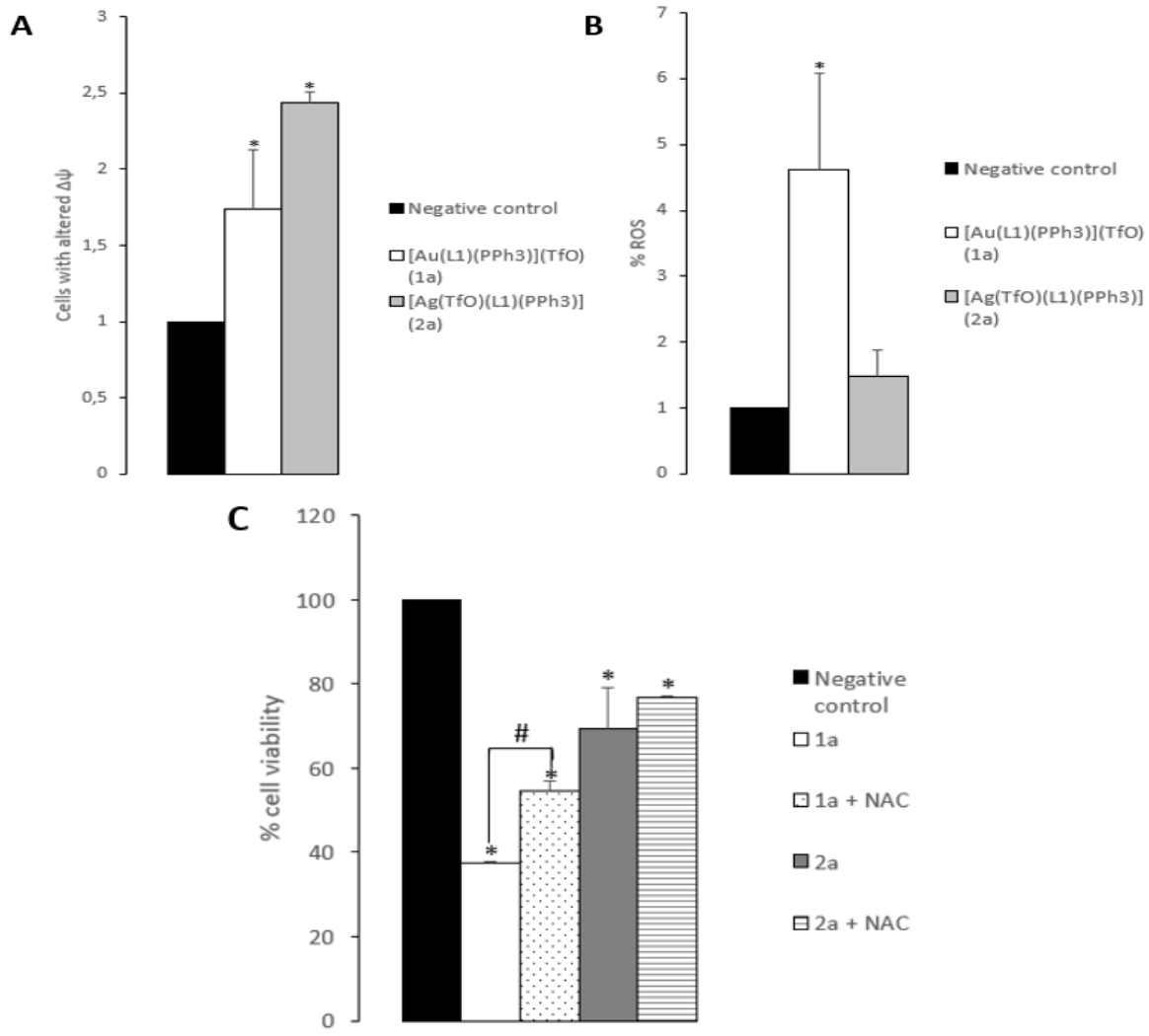

Figure 6. Effect of complexes **1a** and **2a** on mitochondrial integrity and ROS levels of Caco-2 cells. A) Analysis of mitochondrial membrane potential after 48h incubation with **1a** and **2a** (IC_{50}). *p<0.05 *vs* negative control. B) Measurement of ROS levels after 24h incubation with **1a** and **2a** (IC_{50}). *p<0.05 *vs* negative control. C) Percentage of cell viability after 24h with **1a** and **2a** (IC_{50}) in presence or absence of NAC (1h, 30 mM). *p<0.05 *vs* negative control. #p<0.05 *vs* lack of NAC.

2.3.4. Gold(I) complex inhibits TrxR and 20S proteasome

Redox enzyme thioredoxin reductase (TrxR) is one of the main targets of gold(I) derivatives, given the affinity between the gold atom and the selenocysteine residue located on the active site of the protein.[3] Therefore, we measured TrxR activity on Caco-2 cell lysates after 24h incubation with complex **1a**. We also performed TrxR enzymatic activity assay upon 24h incubation with silver-containing complex **2a**, since some authors have reported that silver(I) might be able to inhibit this redox enzyme.[74] As can be observed on Figure 7A, treatment with the gold derivative **1a** resulted in a significant (p<0.05) decrease in TrxR activity, whereas no changes were observed upon treatment

with the silver compound **2a.** Inhibition of TrxR might be related to the increase in ROS levels found upon treatment with complex **1a** (Figure 7B). In line with this, the lack of TrxR inhibition after treatment with **2a** might be in accordance with the absence of redox homeostasis disturbances and the consequent ROS-independent cell death triggered by the silver(I) complex.

In order to determine whether complex **1a** was able to selectively inhibit TrxR or might interact with further redox enzymes, we analyzed glutathione reductase (GR) activity on Caco-2 cell lysates upon 24h incubation with **1a**. In addition, GR activity was measured on Caco-2 cells treated with complex **2a** to compare the effect of both metallodrugs. Whereas incubation with gold derivative **1a** resulted in no modifications of GR activity, which suggests that this complex might act as a selective TrxR inhibitor, treatment with silver(I) complex **2a** leaded to a great increase in glutathione reductase activity (Figure 7B). Cancer cells might increase GR expression and/or activity as a chemoresistance mechanism in order to avoid cell death.[75] However, our results show how the strong increase in GR activity could break the redox equilibrium by modifying the mitochondrial potential and activating the caspases that lead to apoptosis.

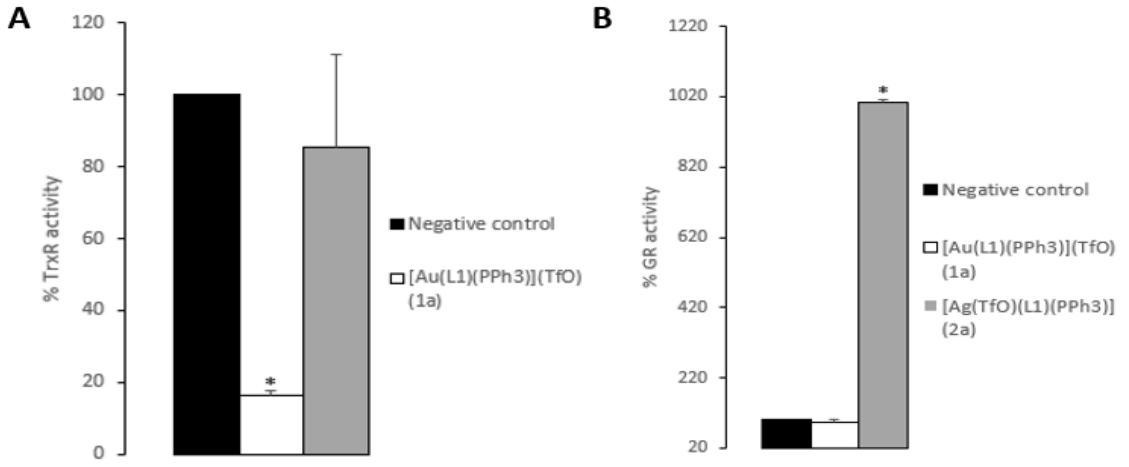

Figure 7. Effect of 24h of treatment with complexes **1a** and **2a** (IC_{50}) on redox enzymes in Caco-2 cells. A) Measurement of thioredoxin reductase activity (TrxR). *p<0.05 *vs* negative control. B) Measurement of glutathione reductase (GR). *p<0.05 *vs* negative control.

Selective TrxR inhibition and the subsequent increase in ROS levels might not be the only mechanism of action of **1a** according to results showed on Figure 6C, since pre-treatment with the ROS scavenger NAC did not fully recover cell viability. Therefore, we hypothesized a likely inhibition of proteasome as a further molecular target, which was feasible according to previous research.[76-77] We measured 20S proteasome activity on

Caco-2 cells treated for 24h with complexes **1a** and **2a** respectively. Incubation with the gold(I) complex **1a** resulted in a significant ($p<0.05$) decrease of chymotrypsin-like activity, thus suggesting that **1a** is able to inhibit 20S proteasome as well as TrxR (Figure 8). Taken together, our results suggest that [Au(L1)(PPh_3)](TfO) (**1a**) might act as a multitarget anticancer complex.

Contrarily, treatment with the silver(I) derivative **2a** triggered an increase in chymotrypsin-like activity, which discards a likely inhibition of proteasome protease capacity as mechanism of action. On the other hand, this unexpected finding might be related with the previously discussed increase in GR activity upon treatment with **2a**, since it has been reported that an increase in proteasomal activity might lead to an overexpression of glutathione reductase along with other antioxidant enzymes.[78]

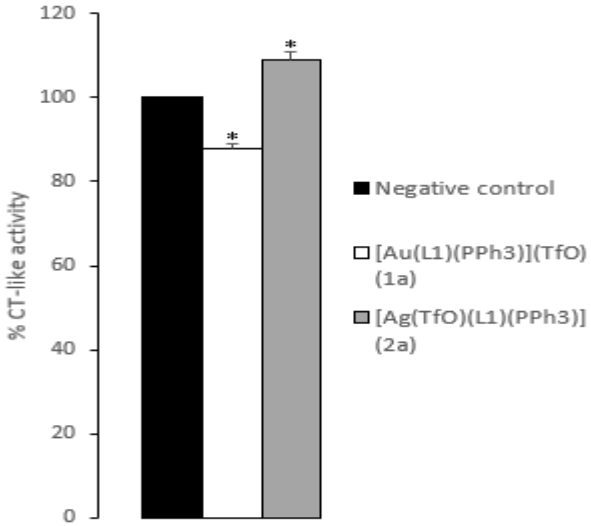

Figure 8. Determination of proteasomal chymotrypsin-like (CT-like) activity on Caco-2 cells upon 24h treatment with complexes **1a** and **2a** (IC_{50}). *$p<0.05$ *vs* negative control.

3. Conclusion

Herein we have described and characterized two heterocyclic ligands derived 2-anilino-pyridine, together with the two families of mononuclear gold(I) and mono- and dinuclear silver(I) derivatives. Both gold-containing complexes [Au(L1)(PPh_3)](TfO) **(1a**) and [Au(L2)(PPh_3)](TfO) (**1b**) displayed great antiproliferative activity toward a model of colorectal adenocarcinoma (Caco-2 cell line) and two breast adenocarcinoma cancer cell lines (MCF-7 and MDA-231). Furthermore, the complex [Au(L1)(PPh_3)](TfO) **(1a**) induced caspases 8 and 3 activation, loss of mitochondrial membrane potential and ROS-dependent cell death on Caco-2 cells upon 24h incubation. Regarding to its mechanism of action, the complex exhibits a significant inhibition of redox enzyme thioredoxin

reductase as well as 20S proteasome. On the other hand, silver complexes also showed good cytotoxic activity and the effect of the silver(I) analogue [Ag(TfO)(L1)(PPh_3)] (**2a**) on Caco-2 cells was evaluated. This derivative triggered ROS-independent apoptosis mediated by caspase 8 and 3 activation and loss of mitochondrial membrane potential. However, cell death is not mediated either by inhibition of the enzyme thioredoxin reductase or 20S proteasome; instead, the silver-containing drug might disrupt mitochondrial function and increase in the activity of the GR according to our current data. Further studies will be needed to validate this hypothesis. In conclusion, we have observed that these new gold(I) and silver(I) complexes might not be able to interact with the same molecular targets, thus triggering different modes of cell death.

Trying to evaluate the structure activity relationship in these compounds we may conclude that although ligand **L1** is less active than **L2**, their complexes are more active in general and within then those bearing gold and triphenylphosphine are the most active. The silver complexes do not show a clear tendency because of for **L1** the dimeric species with tryphenylphosphine exhibit excellent activities in both cell lines, however for **L2** the complexes bearing two ligands coordinated to the metallic center are the most active.

4. Experimental section.

General. Solvents were used as received without purification or drying. The starting material [Ag(OTf)(PPh_3)][79], [Au(OTf)(PPh_3)] was obtained by reaction of [AuCl(PPh_3)] with Ag(OTf) in dichloromethane and used "in situ". All other reagents were commercially available and used without further purification. ^{1}H, $^{13}C\{^{1}H\}$, ^{19}F, and $^{31}P\{^{1}H\}$, including 2D experiments, were recorded on a Bruker Avance 400 or a Bruker ARX 300 spectrometers. Chemical shifts (δ, ppm) were reported relative to the solvent peaks in the ^{1}H, ^{13}C spectra or external 85 % H_3PO_4 or $CFCl_3$ in ^{31}P or ^{19}F spectra. IR spectra were recorded in the range 4000−200 cm^{-1} on a Perkin-Elmer Spectrum 100 spectrophotometer on solid samples using an ATR accessory. C, H, and N analyses were carried out with a Perkin-Elmer 2400 Series 2 microanalyzer. Mass spectra were recorded on a VG Austopec, with the ESI technique.

*4.1. Synthesis of the ligands {(4-pyCO)N(Ph)(py)} (**L1**) and {(2-(C_4H_4S)CO)N(Ph)(py)} (**L2**).* To a dichloromethane solution (10 mL) of 2-anilinopyridine (0.3404 g, 2 mmol) under argón atmosphere was added NEt_3 (0.2626 g, 2.6 mmol) and 4-chlorocarbonylpyridine (0.3560 g, 2 mmol) or 2-chlorocarbonylthiophene (0.2932 g ,2 mmol). The reaction was stirred for 24h at room temperature. The solution was washed

with a saturated solution of $NaHCO_3$ and then washed with dichloromethane (3x20mL) and dried with anhydrous $MgSO_4$. Then the solution was filtered through Celite and the solution was reduced to minimum volume under vacuum. The addition of n-hexane afforded a white solid which was filtered of and washed with n-hexane.

{(4-pyCO)N(Ph)(py)} (**L1**). White solid in 56% yield. ^{1}H NMR (400 MHz, $(CD_3)_2CO$, 25ºC) δ (ppm) = 8.50 (m, 2H, $H^{2'',6''}$); 8.27 (m, 1H, $H^{6'}$); 7.82 (m, 1H, $H^{4'}$); 7.42 (m, 1H, $H^{3'}$); 7.36 (m, 4H, $H^{3'',5''}$, Ph); 7.29 (m, 3H, Ph); 7.22 (m, 1H, $H^{5'}$) ppm. $^{13}C\{^{1}H\}$ NMR (100 MHz, $(CD_3)_2CO$): δ(ppm) = 156.6 ($C^{2'}$); 150.6 ($C^{2'',6''}$); 149.5 ($C^{6'}$); 145.3 (C^{1}); 143.1 ($C^{4''}$); 139.1 ($C^{4'}$); 130.0 ($C^{2,6}$); 128.9 (C^{4}); 127.9 ($C^{3,5}$); 123.1 ($C^{3'}$); 122.8 ($C^{3'',5''}$); 122.4 ($C^{5'}$) ppm. IR: ν(C=O) 1652 cm^{-1}. Elemental analysis calcd. (%) for $C_{17}H_{13}N_3O$ (275.30): C, 74.17; H, 4.76; N, 15.26; found: C, 74.04; H, 4.26; N, 15.41. MS(ESI^+): $[L1+H]^+$ m/z = 276 (100%); $[2L1+Na]^+$ m/z = 573 (45%).

{(2-(C_4H_4S)CO)N(Ph)(py)} (**L2**). White solid in 52% yield. ^{1}H NMR (400 MHz, $(CD_3)_2CO$, 25ºC) δ (ppm) = 8.38 (m, 1H, $H^{6'}$); 7.85 (m, 1H, $H^{4'}$); 7.62 (dd, 1H, J_{H-H} = 5.0; 1.2 Hz, $H^{5''}$); 7.51 (m, 1H, $H^{3'}$); 7.42 (m, 2H, $H^{2,6}$); 7.33 (m, 3H, $H^{3,4,5}$); 7.27 (m, 1H, $H^{5'}$); 6.91 (m, 1H, $H^{4''}$); 6.82 (dd, 1H, J_{H-H} = 3.8;1.2 Hz, $H^{3''}$) ppm. $^{13}C\{^{1}H\}$ NMR (100 MHz, $(CD_3)_2CO$): δ(ppm) = 150.1 ($C^{6'}$); 139.3 ($C^{4'}$); 133.4 ($C^{3''}$); 132.6 ($C^{5''}$); 130.4 ($C^{2,6}$); 129.8 (C^{4}); 128.5 ($C^{3,5}$); 128.2 ($C^{4''}$); 123.4 ($C^{3'}$); 123.2 ($C^{5'}$) ppm. IR: ν(C=O) 1655 cm^{-1}. Elemental analysis calcd. (%) for $C_{16}H_{12}N_2OS$ (280.34): C, 68.55; H, 4.31; N, 9.99; S, 11.44; found: C, 67.84; H, 4.21; N, 9.92; S, 10.87. MS(ESI^+): $[L1+H]^+$ m/z = 276 (100%); $[2L1+Na]^+$ m/z = 573 (45%). MS(ESI+): $[L2+H]^+$ m/z = 281 (100%).

4.2. Synthesis of the complexes [Au(L)(PPh_3)](OTf) (L1, ***1a****; L2,* ***1b****).* To a dichloromethane solution (10 mL) of [AuCl(PPh_3)] (0.1484 g, 0.3 mmol) was added [Ag(OTf)] (0.0848 g, 0.33 mmol). After 45min of stirring protected from light, the white solid (AgCl) was filtered through Celite and the solution was added to dichloromethane solution (10 mL) of L1 (0.0743 g, 0.27 mmol) or L2 (0.0757 g, 0.27 mmol). The reaction was stirred for 2h at room temperature. Then the solution was reduced to minimum volume under vacuum. A white solid was obtained and washed with n-hexane.

*[Au(L1)(PPh_3)](OTf) (****1a****).* White solid in 91% yield. ^{1}H NMR (400 MHz, $(CD_3)_2CO$, 25ºC) δ (ppm) = 8.86 (d, 2H, J_{H-H} = 5.8 Hz, $H^{2'',6''}$); 8.32 (m, 1H, $H^{6'}$); 7.90 (m, 1H, $H^{4'}$); 7.82 (d, 2H, J_{H-H} = 6.0 Hz, $H^{3'',5''}$); 7.65 (m, 15H, PPh_3); 7.49 (d, 1H, J_{H-H} = 8.1 Hz, $H^{3'}$); 7.43 (m, 2H, Ph); 7.35 (m, 3H, Ph); 7.31 (m, 1H, $H^{5'}$) ppm. $^{19}F\{^{1}H\}$ NMR (100 MHz, $(CD_3)_2CO$): δ(ppm) = -80.1 (s). $^{31}P\{^{1}H\}$ NMR (100 MHz, $(CD_3)_2CO$): δ(ppm) = 29.9 (s). $^{13}C\{^{1}H\}$

NMR (100 MHz, $(CD_3)_2CO$): δ(ppm) = δ: 152.5 ($C^{2'',6''}$); 149.9 ($C^{6'}$); 142.2 (s); 135.2 (d, 6C, J_{C-C} = 13.7 Hz, PPh_3); 133.6 (m, 3C, PPh_3); 130.6 (d, 6C, J_{C-C} = 12.1 Hz, PPh_3); 130.3 ($C^{2,6}$); 129.0 (C^4); 128.7 ($C^{3,5}$); 128.1 (s); 125.8 ($C^{3'',5''}$); 123.6 (s, $C^{3'}$ or $C^{5'}$) ppm. IR: ν(C=O) 1653 cm^{-1}, $\nu_{as}(SO_3)$ 1261; $\nu_s(CF_3)$ 1220; $\nu_{as}(CF_3)$ 1143; $\nu_s(SO_3)$ 1030. Elemental analysis calcd. (%) for $C_{36}H_{28}AuF_3N_3O_4PS$ (883.63): C, 48.93; H, 3.19; N, 4.76; S, 3.63; found: C, 48.33; H, 2.96; N, 4.38; S, 3.24. MS(ESI+): $[L1+H]^+$ m/z = 276 (100%); $[M-OTf]^+$ m/z = 734 (17%); $[Au(PPh_3)_2]^+$ m/z = 721 (65%).

*[Au(L2)(PPh₃)](OTf) (**1b**).* White solid in 60% yield. ^1H NMR (400 MHz, $(CD_3)_2CO$, 25ºC) δ (ppm) = 9.09 (m, 1H, $H^{6'}$); 8.48 (td, 1H, J_{H-H} = 7.9; 1.7 Hz, $H^{4'}$); 7.94 (m, 2H, $H^{3',5'}$); 7.66-7.44 (m, 21H, $H^{5''}$+PPh_3); 6.81 (dd, 1H, J_{H-H} = 3.9; 1.2 Hz, $H^{3''}$); 6.76 (m, 1H, $H^{4''}$) ppm. $^{19}F\{^1H\}$ NMR (100 MHz, $(CD_3)_2CO$): δ(ppm) = -80.1 (s). $^{31}P\{^1H\}$ NMR (100 MHz, $(CD_3)_2CO$): δ(ppm) = 30.1 (s). $^{13}C\{^1H\}$ NMR (100 MHz, $(CD_3)_2CO$): δ(ppm) = δ: 164.51 (s, 1C, C=O); 156.9 (s); 152.6 ($C^{6'}$); 145.3 ($C^{4'}$); 142.3 (s); 137.5 (s); 135.0 (d, 6C, J_{C-C} = 13.6 Hz, PPh_3); 134.7 ($C^{3''}$); 134.3 ($C^{5'}$); 133.5 (m, 2C, PPh_3); 131.0 ($C^{2,6}$); 130.5 (d, 6C, J_{C-C} = 12.1 Hz, PPh_3); 129.7 (C^4); 129.1 ($C^{3,5}$); 128.5 ($C^{4''}$); 127.6 ($C^{3'}$); 126.0 ($C^{5'}$) ppm.. IR: ν(C=O) 1631 cm^{-1}, $\nu_{as}(SO_3)$ 1257; $\nu_s(CF_3)$ 1225; $\nu_{as}(CF_3)$ 1150; $\nu_s(SO_3)$ 1029. Elemental analysis calcd. (%) for $C_{35}H_{27}AuF_3N_2O_4PS_2$ (888.67): C, 47.30; H, 3.06; N, 3.15; S, 7.22; found: C, 47.8; H, 2.93; N, 3.62; S, 6.94. MS(ESI+): $[L2+H]^+$ m/z = 281 (8%); $[Au(PPh_3)_2]^+$ m/z = 721 (100%).

*4.3. Synthesis of the complexes [Ag(OTf)(L)(PPh₃)] (L1, **2a**; L2, **2b**).* To a dichloromethane solution (10 mL) of $[Ag(OTf)(PPh_3)]$ (0.1557 g, 0.3 mmol) was added L1 or L2 (0.3 mmol). After 45min of stirring protected from light at room temperature, the solution was reduced to minimum volume under vacuum. A white solid was obtained and washed with n-hexane.

*[Ag(OTf)(L1)(PPh₃)] (**2a**).* White solid in 52% yield. ^1H NMR (400 MHz, $(CD_3)_2CO$, 25ºC) δ (ppm) = 8.66 (m, 2H, $H^{2'',6''}$); 8.34 (m, 1H, $H^{6'}$); 7.89 (m, 1H, $H^{4'}$); 7.55 (m, 17H, $H^{3'',5''}$+PPh_3); 7.48 (d, 1H, J_{H-H} = 8.1 Hz, $H^{3'}$); 7.39 (m, 2H, Ph); 7.33 (m, 4H, H^5+Ph) ppm. $^{19}F\{^1H\}$ NMR (100 MHz, $(CD_3)_2CO$): δ(ppm) = -77.9 (s). $^{31}P\{^1H\}$ NMR (100 MHz, $(CD_3)_2CO$, 203 K): δ(ppm) = 13.7 (2d, $J_{109Ag-P}$ = 762.8 Hz, $J_{107Ag-P}$ = 661.0 Hz, $AgPPh_3$) ppm. $^{13}C\{^1H\}$ NMR (100 MHz, $(CD_3)_2CO$): δ(ppm) = δ: 156.3 (s); 151.8 ($C^{2'',6''}$); 149.9 ($C^{6'}$); 142.6 (m); 139.7 ($C^{4'}$); 134.8 (d, 6C, J_{C-C} = 15.8 Hz, PPh_3); 132.1 (3C, PPh_3); 131.4 (d, 3C, J_{C-C} = 41.4 Hz, PPh_3); 130.2 (m, 6C, PPh_3); 130.2 ($C^{2,6}$); 128.9 (C^4); 128.3 ($C^{3,5}$); 123.2 ($C^{3'',5''}$); 122.7 ($C^{3',5'}$) ppm IR: ν(C=O) 1635 cm^{-1}, $\nu_{as}(SO_3)$ 1246; $\nu_s(CF_3)$ 1224;

$\nu_{as}(CF_3)$ 1145; $\nu_s(SO_3)$ 1026. Elemental analysis calcd. (%) for $C_{36}H_{28}AgF_3N_3O_4PS$ (794.53): C, 54.42; H, 3.55; N, 5.29, S, 4.04; found: C, 54.47; H, 3.71; N, 5.18; S, 4.44. MS(ESI+): $[Ag(PPh_3)_2]^+$ m/z = 633 (100%); $[M\text{-}OTf]^+$ m/z = 646 (25%).

*[Ag(OTf)(L2)(PPh$_3$)] (**2b**).* White solid in 68% yield. ^{1}H NMR (400 MHz, $(CD_3)_2CO$, 25ºC) δ (ppm) = 8.39 (m, 1H, H$^{6'}$); 7.87 (m, 1H, H$^{4'}$); 7.63 (dd, 1H, $J_{H\text{-}H}$ = 5.0; 1.2 Hz, H$^{5''}$); 7.57 (m, 3H, H$^{2,6,3'}$); 7.47 (m, 15H, PPh_3); 7.34 (m, 3H, H^{3,4,5}); 7.28 (m, 1H, H$^{5'}$); 6.91 (m, 1H, H$^{4''}$); 6.82 (dd, 1H, $J_{H\text{-}H}$ = 3.8; 1.2 Hz, H$^{3''}$) ppm ^{19}F{^{1}H} NMR (100 MHz, $(CD_3)_2CO$): δ(ppm) = -78.7 (s). ^{31}P{^{1}H} NMR (100 MHz, $(CD_3)_2CO$, 203 K): δ(ppm) = 10.1 (2m, 1P, $J_{109Ag\text{-}P}$ = 533.3 Hz, $J_{107Ag\text{-}P}$ = 463.1 Hz) ppm. ^{13}C{^{1}H} NMR (100 MHz, $(CD_3)_2CO$): δ(ppm) = 149.9 (s); 139.2 (s); 134.7 (d, 6C, $J_{C\text{-}C}$ = 15.5 Hz, PPh_3); 133.2 (s); 132.3 (s); 132.0 (s, 3C, PPh_3); 131.5 (s); 130.2 (s, 6C, PPh_3); 129.4 (s); 128.2 (s); 127.8 (s); 123.2 ppm. IR: ν(C=O) 1625 cm^{-1}, $\nu_{as}(SO_3)$ 1265; $\nu_s(CF_3)$ 1221; $\nu_{as}(CF_3)$ 1141; $\nu_s(SO_3)$ 1026. Elemental analysis calcd. (%) for $C_{35}H_{27}AgF_3N_2O_4PS_2$ (799.57): C, 52.58; H, 3.40; N, 3.50; S, 8.02.; found: C, 52.30; H, 3.41; N, 3.23; S, 8.34. MS(ESI+): $[Ag(PPh_3)_2]^+$ m/z = 633 (100%); $[M\text{-}OTf]^+$ m/z = 651 (13%).

*4.4. Synthesis of the complexes [Ag$_2$(OTf)$_2$(L)(PPh$_3$)$_2$] (L1, **3a**; L2, **3b**).* To a dichloromethane solution (10 mL) of [Ag(OTf)(PPh$_3$)] (0.1557 g, 0.6 mmol) was added L1 or L2 (0.3 mmol). After 45min of stirring protected from light at room temperature, the solution was reduced to minimum volume under vacuum. A white solid was obtained and washed with n-hexane.

*[Ag$_2$(OTf)$_2$(L1)(PPh$_3$)$_2$] (**3a**).* White solid in 78% yield. ^{1}H NMR (400 MHz, $(CD_3)_2CO$, 25ºC) δ (ppm) = 8.71 (m, 2H, H$^{2'',6''}$); 8.47 (m, 1H, H$^{6'}$); 7.96 (m, 1H, H$^{4'}$); 7.54 (m, 33H, H$^{3',3'',5''}$+PPh_3); 7.35 (m, 5H, Ph); 7.27 (m, 1H, H$^{5'}$) ppm. ^{19}F{^{1}H} NMR (100 MHz, $(CD_3)_2CO$): δ(ppm) = -79.9 (s). ^{31}P{^{1}H} NMR (100 MHz, $(CD_3)_2CO$, 203 K): δ(ppm) = 13.1 (2d, $J_{109Ag\text{-}P}$ = 927.9 Hz, $J_{107Ag\text{-}P}$ = 838.8 Hz, $AgPPh_3$) ppm. ^{13}C{^{1}H} NMR (100 MHz, $(CD_3)_2CO$): δ(ppm) = δ: 152.1 (C$^{2'',6''}$); 150.4 (C$^{6'}$); 142.6 (m); 140.3 (C$^{4'}$); 134.8 (m, 12C, PPh_3); 132.1 (6C, PPh_3); 130.4 (C^{2,6}); 130.2(m, 12C, PPh_3); 128.8 (C^4); 128.5 (C^{3,5}); 124.5 (py); 123.5 (py); 123.4 (py) ppm IR: ν(C=O) 1667 cm^{-1}, $\nu_{as}(SO_3)$ 1239; $\nu_s(CF_3)$ 1220; $\nu_{as}(CF_3)$ 1149; $\nu_s(SO_3)$ 1023. Elemental analysis calcd. (%) for $C_{55}H_{43}Ag_2F_6N_3O_7P_2S_2$ (1313.75): C, 50.28; H, 3.30; N, 3.20; S, 4.88; found: C, C, 50.68; H, 3.62; N, 3.43; S, 4.35. MS(ESI+): $[Ag(PPh_3)_2]^+$ m/z = 633 (100%); $[M\text{-}Ag\text{-}2OTf]^+$ m/z = 646 (50%).

*$[Ag_2(OTf)_2(L2)(PPh_3)_2]$ (**3b**).* White solid in 44% yield. ^{1}H NMR (400 MHz, $(CD_3)_2CO$, 25ºC) δ (ppm) = 8.62 (m, 1H, $H^{6'}$); 8.04 (m, 1H, $H^{4'}$); 7.58 (m, 32H, $H^{3',5''}$+PPh_3); 7.47 (m, 1H, $H^{5'}$); 7.39 (m, 4H, Ph); 7.36 (m, 1H, Ph); 6.85 (m, 1H, $H^{4''}$); 6.78 (dd, 1H, J_{H-H} = 3.8 1.2 Hz, $H^{3''}$) ppm. ^{19}F{^{1}H} NMR (100 MHz, $(CD_3)_2CO$): δ(ppm) = -80 (s). ^{31}P{^{1}H} NMR (100 MHz, $(CD_3)_2CO$, 203 K): δ(ppm) = 13.0 (2m, 1P, $J_{Ag-P\ (average)}$ = 725.5 Hz, $SAgPPh_3$); 10.6 (2m, $J_{Ag-P\ (average)}$ = 520.9 Hz, $NAgPPh_3$) ppm. ^{13}C{^{1}H} NMR (100 MHz, $(CD_3)_2CO$): δ(ppm) = 151.4 ($C^{6'}$); 141.7 ($C^{4'}$); 134.8 (m, 6C, PPh_3); 134.0 ($C^{3''}$); 133.3 ($C^{5''}$); 132.1 (s, 3C, PPh_3); 130.7 (s, 2C, $C^{2,6}$); 130.2 (s, 6C, PPh_3); 129.1 (C^4); 129.0 (s, 2C, $C^{3,5}$); 128.1 ($C^{4''}$); 125.0 ($C^{3'}$); 124.0 ($C^{5'}$) ppm. IR: ν(C=O) 1638 cm^{-1}, $\nu_{as}(SO_3)$ 1239; $\nu_s(CF_3)$ 1220; $\nu_{as}(CF_3)$ 1148; $\nu_s(SO_3)$ 1023. Elemental analysis calcd. (%) for $C_{54}H_{42}Ag_2F_6N_2O_7P_2S$ (1318.79): C, 49.18; H, 3.21; N, 2.12; S, 7.29; found: C, 49.01; H, 3.25; N, 1.99; S, 6.98. MS(ESI+): $[Ag(PPh_3)_2]^+$ m/z = 633 (100%); $[L2+Ag(PPh_3)]^+$ m/z = 651 (61%).

*4.5. Synthesis of the complexes $[Ag(OTf)(L)]_2$ (L1, **4a**; L2, **4b**).* To a dichloromethane solution (10 mL) of [Ag(OTf)] (0.051 g, 0.2 mmol) was added L1 or L2 (0.2 mmol). After 45min of stirring protected from light at room temperature, the solution was reduced to minimum volume under vacuum. A white solid was obtained and washed with n-hexane.

*$[Ag(OTf)(L1)]_2$ (**4a**).* White solid in 72% yield. ^{1}H NMR (400 MHz, $(CD_3)_2CO$, 25ºC) δ (ppm) = 8.56 (m, 4H, $H^{2'',6''}$); 8.30 (m, 2H, $H^{6'}$); 7.86 (td, 2H, J_{H-H} = 7.9; 2.0 Hz, $H^{4'}$); 7.45 (m, 6 H, $H^{3',3'',5''}$); 7.39 (m, 4H, *Ph*); 7.29 (m, 8H, $H^{5'}$+Ph) ppm. ^{19}F{^{1}H} NMR (100 MHz, $(CD_3)_2CO$): δ(ppm) = -77.8 (s). ^{13}C{^{1}H} NMR (100 MHz, $(CD_3)_2CO$): δ(ppm) = δ: 168.0 (s, 2C, C=O); 154.8 (s, 2C); 149.9 (4C, $C^{2'',6''}$); 148.8 ($C^{6'}$); 144.6 (s, 2C); 141.1 (s, 2C); 138.8 (s, 2C, $C^{4'}$); 129.3 (s, 4C, $C^{2,6}$); 128.0 (C^4); 122.7 ($C^{3',5'}$); 122.6 (s, 2C); 122.4 (s, 2C); 121.9 (s,2C). IR: ν(C=O) 1659 cm^{-1}, $\nu_{as}(SO_3)$ 1248; $\nu_s(CF_3)$ 1221; $\nu_{as}(CF_3)$ 1141; $\nu_s(SO_3)$ 1026. Elemental analysis calcd. (%) for $C_{36}H_{26}Ag_2F_6N_6O_8S_2$ (1064.48): C, 40.62; H, 2.46; N, 7.89; S, 6.02; found: C, 39.98; H, 2.40; N, 7.81; S, 5.98. MS(ESI+): $[L1+H]^+$ m/z = 276 (100%); $[M-2OTf-Ag]^+$ m/z = 657 (99%); $[M-OTf+Na]^{2+}$ m/z = 938 (8%).

*$[Ag(OTf)(L2)]_2$ (**4b**).* White solid in 16% yield. ^{1}H NMR (400 MHz, $(CD_3)_2CO$, 25ºC) δ (ppm) = 8.88 (m, 2H, $H^{6'}$); 8.52 (M, 2H, $H^{4'}$); 7.86 (m, 4 H, $H^{5',5''}$); 7.71 (m, 10H, *Ph*); 7.38 (d, 2H, J_{H-H} = 8.4 Hz, $H^{3'}$); 7.01 (m, 4H, $H^{3'',4''}$) ppm. ^{19}F{^{1}H} NMR (100 MHz, $(CD_3)_2CO$): δ(ppm) = -80.0 (s). ^{13}C{^{1}H} NMR (100 MHz, $(CD_3)_2CO$): δ(ppm) = δ: 165.3 (s, 2C); 153.1 (s, 2C); 147.0 (s, 2C, $C^{4'}$); 136.4 and 128.6 (m, 4C, $C^{3'',4''}$); 136.0 (s, 2C,

$C^{5'}$ or $C^{5''}$), 131.9 (s, 4C, $C^{2,6}$); 131.6 (C^4); 130.7 (s, 4C, $C^{3,5}$) ppm. IR: ν(C=O) 1644 cm^{-1}, $\nu_{as}(SO_3)$ 1256; $\nu_s(CF_3)$ 1221; $\nu_{as}(CF_3)$ 1146; $\nu_s(SO_3)$ 1023. Elemental analysis calcd. (%) for $C_{34}H_{24}Ag_2F_6N_4O_8S_4$ (1074.56): C, 38.00; H, 2.25; N, 5.21; S, 11.94; found: C, 38.28; H, 2.20; N, 4.88; S, 11.99. MS(ESI+): $[L2+H]^+$ m/z = 281 (100%).

*4.6. Synthesis of the complexes [Ag(OTf)(L)$_2$] (L1, **5a**; L2, **5b**).* To a dichloromethane solution (10 mL) of [Ag(OTf)] (0.051 g, 0.2 mmol) was added L1 or L2 (0.4 mmol). After 45min of stirring protected from light at room temperature, the solution was reduced to minimum volume under vacuum. A white solid was obtained and washed with n-hexane.

*[Ag(OTf)(L1)$_2$] (**5a**).* White solid in 54% yield. ^{1}H NMR (400 MHz, $(CD_3)_2CO$, 25ºC) δ (ppm) = 8.54 (m, 4H, $H^{2'',6''}$); 8.28 (m, 2H, $H^{6'}$); 7.83 (m, 2H, $H^{4'}$); 7.39 (m, 10 H, $H^{3',3'',5''}$ + *Ph*); 7.28 (m, 6H, Ph); 7.23 (td, 2H, J_{H-H} = *4.9; 1.0 Hz*, $H^{5'}$) ppm. $^{19}F\{^1H\}$ NMR (100 MHz, $(CD_3)_2CO$): δ(ppm) = -78.9 (s). $^{13}C\{^1H\}$ NMR (100 MHz, $(CD_3)_2CO$): δ(ppm) = δ: 150.5 (4C, $C^{2'',6''}$); 149.6 ($C^{6'}$); 139.3 (s, 2C, $C^{4'}$); 130.1 (s, 4C, $C^{2,6}$); 129.0 (C^4); 128.1 (s, 4C, $C^{3,5}$); 123.8 (s, 4C, $C^{3'',5''}$); 122.9 (s, 2C, $C^{3'}$); 122.4 (s, 2C, $C^{5'}$) ppm. IR: ν(C=O) 1654 cm^{-1}, $\nu_{as}(SO_3)$ 1251; $\nu_s(CF_3)$ 1222; $\nu_{as}(CF_3)$ 1154; $\nu_s(SO_3)$ 1027. Elemental analysis calcd. (%) for C35H26AgF3N6O5S (807.55): C, 52.06; H, 3.25; N, 10.41; S, 3.97; found: C, 52.55; H, 3.23; N, 10.39; S, 3.56. MS(ESI+): $[L1+H]^+$ m/z = 276 (45%); $[M\text{-}OTf]^+$ m/z = 659 (100%).

*[Ag(OTf)(L2)$_2$] (**5b**).* White solid in 39% yield. ^{1}H NMR (400 MHz, $(CD_3)_2CO$, 25ºC) δ (ppm) = 8.51 (m, 2H, $H^{6'}$); 8.12 (m, 2H, $H^{4'}$); 7.56 (d, 2 H, J_{H-H} = 4.4 Hz, $H^{5''}$); 7.47 (m, 14H, $H^{3',5'}$ + *Ph*); 6.90 (m, 4H, $H^{3'',4''}$) ppm. $^{19}F\{^1H\}$ NMR (100 MHz, $(CD_3)_2CO$): δ(ppm) = -80.1 (s). $^{13}C\{^1H\}$ NMR (100 MHz, $(CD_3)_2CO$): δ(ppm) = δ: 133.7 (s, 2C, $C^{5'}$), 130.9 (s, 4C, $C^{2,6}$); 129.5 (s, 2C, C^4); 129.4 (s, 4C, $C^{3,5}$); 128.2 (s, 2C, $C^{4'}$) ppm. IR: ν(C=O) 1646 cm^{-1}, $\nu_{as}(SO_3)$ 1258; $\nu_s(CF_3)$ 1222; $\nu_{as}(CF_3)$ 1150; $\nu_s(SO_3)$ 1027. Elemental analysis calcd. (%) for $C_{33}H_{24}AgF_3N_4O_5S_3$ (817.63): C, 48.48; H, 2.96; N, 6.85; S, 11.77; found: C, 48.52; H, 3.03; N, 6.92; S, 12.24. MS(ESI+): $[L2+H]^+$ m/z = 281 (100%); $[M\text{-}TfO]^+$ m/z = 669 (1%); $[M+H]^+$ m/z = 819 (1%);

4.7. Cell culture

Human colorectal adenocarcinoma Caco-2 cells were kindly provided by Dr. Edith Brot-Laroche (Université Pierre et Marie Curie-Paris 6 UMR S872, Les Cordeliers, France). Human breast adenocarcinoma MCF-7 and MDA-231 cells were kindly provided by Carlos J. Ciudad and Dr. Verònica Noé (Departamento de Bioquímica y Fisiología, Facultad de Farmacia, Universidad de Barcelona, Spain). All cell lines were maintained

in a humidified atmosphere of 5% CO_2 at 37ºC. Cells (passages 20-40) were grown in Dulbecco's Modified Eagles medium (DMEM) (Gibco Invitrogen, Paisley, UK) supplemented with 20% fetal bovine serum, 1% non-essential amino acids, 1% penicillin (1000 U/mL), 1% streptomycin (1000 μg/mL) and 1% amphotericin (250 U/mL). Culture medium was replaced every two days and cells were passaged enzymatically with 0.25% trypsin-1 mM EDTA and sub-cultured on 25 cm^2 flasks at a density of $2 \cdot 10^4$ cells/cm^2. Experiments in undifferentiated Caco-2 cells as well as on MCF-7 and MDA-231 cells were performed 24h post-seeding. For assays on differentiated Caco-2 cells, cells were cultured on 96-wells plates under standard culture conditions for 7 to 9 days, until reaching 80% confluence as confirmed by optic microscopy observance.

4.8. Cell treatment. Complexes were initially solved on DMSO to a concentration of 20 mM and then diluted on cell culture without fetal bovine serum to the required work concentrations. For treatment, cell culture medium was replaced with medium containing complexes and cells were incubated at 37ºC for a variable time depending on the assay.

4.9. Cell proliferation assay and IC_{50} calculation. MTT assay was performed as previously described by Mármol *et al*.[59]

For IC_{50} calculation, cells were grown in 96-wells plates at a density of 4000 cells per well and incubated overnight at standard culture conditions. Then, cells were exposed to a range of concentrations of complexes (0-20 μM for complexes **1-5a** and **1-5b**; 10-100 μM for coordination ligands **L1** and **L2**) for 72h. Changes in cell proliferation were analysed by MTT and the obtained absorbance values were converted into percentage of growth inhibition. Absorbance was measured with SPECTROstar Nano (BMG Labtech).

4.10. Cell death studies. Caco-2 cells were grown at 25 cm^2 flasks at a density of 300.000 cells per flask and incubated overnight under standard culture conditions. Cells were then exposed to gold and silver complexes for 48h, then collected and stained with Annexin V-FITC by flow cytometry as previously described by Sánchez-de-Diego *et al*.[80]

4.10. Measurement of caspase 8 and caspase 3 activation. Caco-2 cells were grown at 25 cm^2 flasks at a density of 300.000 cells per flask and incubated overnight under standard culture conditions. Cells were then exposed to gold and silver complexes for 24h and collected for caspase 8 and 3 activity measurement.

Caspase 8 Assay Kit (Abcam; ab39700) was used for colorimetric determination of caspase 8 activation. Treated Caco-2 cells were manipulated according to manufacturer's instructions and absorbance was measured at 400 nm with SPECTROstar Nano (BMG Labtech). Protein concentration was determined by Bradford method.

For caspase 3 activation measurement, *Caspase 3Assay Kit, Colorimetric* (Sigma-Aldrich; CASP-3-C) was used. Treated Caco-2 cells were manipulated according to manufacturer's instructions and absorbance was measured at 405 nm with SPECTROstar Nano (BMG Labtech). Protein concentration was determined by Bradford method.

4.11. Propidium iodide staining of DNA content and cell cycle analysis. Caco-2 cells were grown at 25 cm^2 flasks at a density of 300.000 cells per flask and incubated overnight under standard culture conditions. Cells were exposed to gold and silver complexes for 48h, then collected and changes in cell cycle were analyzed as previously described by Sánchez-de-Diego *et al*.[80]

4.12. Flow cytometry mitochondrial membrane potential assay. Caco-2 cells were grown at 25 cm^2 flasks at a density of 300.000 cells per flask and incubated overnight under standard culture conditions. Cells were then exposed to gold and silver complexes for 48h and changes in $\Delta\psi$ were performed as previously described by Sánchez-de-Diego *et al*.[80]

4.13. Analysis of total cellular oxidative stress. Caco-2 cells cells were grown in 96-wells plates at a density of 4000 cells per well, and after overnight incubation under standard culture conditions, were exposed to gold and silver complexes 24h. Thereafter, measurement of total intracellular ROS levels was performed as previously described by Sánchez-de-Diego *et al*.[80] Fluorescence data were normalized with percentage of cell viability determined by MTT.

4.14. Analysis of thioredoxin reductase activity. Caco-2 cells cells were grown in 96-wells plates at a density of 4000 cells per well, and after overnight incubation under standard culture conditions, were exposed to gold and silver complexes 24h. Then, TrxR activity was determined as previously described by Mármol *et al*.[59] Absorbance was measured with SPECTROstar Nano (BMG Labtech).

4.15. Measurement of glutathione reductase activity. Caco-2 cells cells were grown in 96-wells plates at a density of 4000 cells per well, and after overnight incubation under standard culture conditions, were exposed to gold and silver complexes for 24h. Analysis of GR activity was performed as previously described by Sánchez-de-Diego *et al*.[80] Absorbance was measured with SPECTROstar Nano (BMG Labtech).

4.16. Analysis of 20S proteasome activity. Caco-2 cells were grown at 25 cm^2 flasks at a density of 300.000 cells per flask and incubated overnight under standard culture conditions. Cells were exposed to gold and silver complexes for 24h, then collected and lysed with saponine and centrifuged at 13.000 rpm for 15 min at 4ºC. Supernatant was further analyzed with *Proteasome 20S Activity Assay Kit* (Sigma-Aldrich; MAK172)

according manufacturer's instructions. Fluorescence was measured with FLUOstar Omega (BMG Labtech).

4.17. Crystal Structure Determinations

Crystals were mounted in inert oil on glass fibres and transferred to the cold gas stream of a Smart APEX CCD diffractometers equipped with a low-temperature attachment. Data were collected using monochromated MoKα radiation (λ = 0.71073 Å). Scan type ϖ. Absorption corrections based on multiple scans were applied using SADABS.[75] The structures were solved by direct methods and refined on F^2 using the program SHELXT-2016.[76] All non-hydrogen atoms were refined anisotropically. CCDC deposition numbers 2020939 (**L1**), 2020940 (**L2**), 2020941 (**1a**), and 2020942 (**1b**) contain the supplementary crystallographic data. These data can be obtained free of charge by The Cambridge Crystallography Data Center.

Conflicts of interest

Authors declare no conflict of interest.

Acknowledgments

Authors thank to Centro de Investigación Biomédica de Aragón (CIBA), España for technical assistance: http://www.iacs.aragon.es, use of Servicio General de Apoyo a la Investigación-SAI, Universidad de Zaragoza. We thank The Ministerio de Economía y Competitividad (CTQ2016-75816-C2-1-P, PID2019-104379RB-C21 and SAF2016-75441-R), CIBEROBN under Grant (CB06/03/1012) of the Instituto Carlos III, European Grant Interreg/SUDOE (Redvalue, SOE1/PI/E0123), Red Multimetdrugs (RED2018-102471-T) and Aragon Regional Government (B16_R17 and E07_20R) for financial support.

Associated content

Supporting Information

RMN spectra of all the complexes are included in the supporting information.

Abbreviations

Apoptosis-inducing factor: AIF

Cyclooxygenase-2: COX-2

Dulbecco's Modified Eagles medium: DMEM

Glutathione reductase: GR

Lipoxygenase: LOX

Mitochondrial membrane potential: Δψ

N-acetyl-cysteine: NAC

N-heterocyclic carbene: NHC

Reactive oxygen species: ROS

Selective Index: SI

References

1. Rabik, C. A.; Dolan, M. E., Molecular mechanisms of resistance and toxicity associated with platinating agents. *Cancer Treat. Rev.* **2007,** *33*, 9-23.
2. Kelland, L., The resurgence of platinum-based cancer chemotherapy. **2007,** *7*, 573-584.
3. Bindoli, A.; Rigobello, M. P.; Scutari, G.; Gabbiani, C.; Casini, A.; Messori, L., Thioredoxin reductase: A target for gold compounds acting as potential anticancer drugs. *Coord. Chem. Rev.* **2009,** *253* (11-12), 1692-1707.
4. McKeage, M. J.; Maharaj, L.; Berners-Price, S. J., Mechanisms of cytotoxicity and antitumor activity of gold(I) phosphine complexes: the possible role of mitochondria. *Coord. Chem. Rev.* **2002,** *232* (1-2), 127-135.
5. de Almeida, A.; Oliveira, B. L.; Correia, J. D. G.; Soveral, G.; Casini, A., Emerging protein targets for metal-based pharmaceutical agents: An update. *Coord. Chem. Rev.* **2013,** *257* (19-20), 2689-2704.
6. Estrada-Ortiz, N.; Guarra, F.; de Graaf, I. A. M.; Marchetti, L.; de Jager, M. H.; Groothuis, G. M. M.; Gabbiani, C.; Casini, A., Anticancer Gold N-Heterocyclic Carbene Complexes: A Comparative in vitro and ex vivo Study. *ChemMedChem* **2017,** *12* (17), 1429-1435.
7. Pratesi, A.; Cirri, D.; Durovic, M. D.; Pillozzi, S.; Petroni, G.; Bugarcic, Z. D.; Messori, L., New gold carbene complexes as candidate anticancer agents. *Biometals* **2016,** *29* (5), 905-911.
8. Liu, W. K.; Gust, R., Update on metal N-heterocyclic carbene complexes as potential anti-tumor Metallodrugs. *Coord. Chem. Rev.* **2016,** *329*, 191-213.
9. Zhang, X. N.; Selvaraju, K.; Saei, A. A.; D'Arcy, P.; Zubarev, R. A.; Arner, E. S. J.; Linder, S., Repurposing of auranofin: Thioredoxin reductase remains a primary target of the drug. *Biochimie* **2019,** *162*, 46-54.
10. Mora, M.; Gimeno, M. C.; Visbal, R., Recent advances in gold-NHC complexes with biological properties. *Chem. Soc. Rev.* **2019,** *48*, 447-462.
11. Mirzadeh, N.; Reddy, T. S.; Bhargava, S. K., Advances in diphosphine ligand-containing gold complexes as anticancer agents. *Coord. Chem. Rev.* **2019,** *388*, 343-359.
12. Marmol, I.; Quero, J.; Rodriguez-Yoldi, M. J.; Cerrada, E.; , Gold as a possible alternative to platinum-based chemotherapy for colon cancer. *Cancers* **2019,** *11*, 780-816.
13. E. Cerrada; V. Fernández-Moreira; Gimeno, M. C., Gold and platinum alkynyl complexes for biomedical applications. In *Advances in Organometallic Chemistry*, Pérez, P., Ed. Elsevier Academic Press: 2019; Vol. 71, pp 227-258.
14. Porchia, M.; Pellei, M.; Marinelli, M.; Tisato, F.; Del Bello, F.; Santini, C., New insights in Au-NHCs complexes as anticancer agents. *Eur. J. Med. Chem.* **2018,** *146*, 709-746.
15. Hussaini, S. Y.; Haque, R. A.; Razali, M. R., Recent progress in silver(I)-, gold(I)/(III)- and palladium(II)-N-heterocyclic carbene complexes: A review towards biological perspectives. *J. Organomet. Chem.* **2019,** *882*, 96-111.
16. Liang, X. X.; Luan, S. X.; Yin, Z. Q.; He, M.; He, C. L.; Yin, L. Z.; Zou, Y. F.; Yuan, Z. X.; Li, L. X.; Song, X.; Lv, C.; Zhang, W., Recent advances in the medical use of silver complex. *Eur. J. Med. Chem.* **2018,** *157*, 62-80.
17. Johnson, N. A.; Southerland, M. R.; Youngs, W. J., Recent Developments in the Medicinal Applications of Silver-NHC Complexes and Imidazolium Salts. *Molecules* **2017,** *22* (8).
18. Medici, S.; Peana, M.; Nurchi, V. M.; Lachowicz, J. I.; Crisponi, G.; Zoroddu, M. A., Noble metals in medicine: Latest advances. *Coord. Chem. Rev.* **2016,** *284*, 329-350.
19. Banti, C. N.; Hadjikakou, S. K., Anti-proliferative and anti-tumor activity of silver(I) compounds. *Metallomics* **2013,** *5* (6), 569-596.

20. Lin, J. C. Y.; Huang, R. T. W.; Lee, C. S.; Bhattacharyya, A.; Hwang, W. S.; Lin, I. J. B., Coinage Metal-N-Heterocyclic Carbene Complexes. *Chem. Rev.* **2009,** *109* (8), 3561-3598.
21. Medici, S.; Peana, M.; Crisponi, G.; Nurchi, V. M.; Lachowicz, J. I.; Remelli, M.; Zoroddu, M. A., Silver coordination compounds: A new horizon in medicine. *Coord. Chem. Rev.* **2007,** *327*, 349-359.
22. Liu, W. K.; Gust, R., Metal N-heterocyclic carbene complexes as potential antitumor metallodrugs. *Chem. Soc. Rev* **2016,** *42* (2), 755-773.
23. Hindi, K. M.; Panzner, M. J.; Tessier, C. A.; Cannon, C. L.; Youngs, W. J., The Medicinal Applications of Imidazolium Carbene-Metal Complexes. *Chem. Rev.* **2009,** *109* (8), 3859-3884.
24. Kascatan-Nebioglu, A.; Panzner, M. J.; Tessier, C. A.; Cannon, C. L.; Youngs, W. J., N-Heterocyclic carbene-silver complexes: A new class of antibiotics. *Coord. Chem. Rev.* **2007,** *251* (5-6), 884-895.
25. Mercs, L.; Albrecht, M., Beyond catalysis: N-heterocyclic carbene complexes as components for medicinal, luminescent, and functional materials applications. *Chem. Soc. Rev* **2010,** *39* (6), 1903-1912.
26. Patra, M.; Gasser, G.; Metzler-Nolte, N., Small organometallic compounds as antibacterial agents. *Dalton Trans.* **2012,** *41* (21), 6350-6358.
27. Lansdown, A. B. G., A Pharmacological and Toxicological Profile of Silver as an Antimicrobial Agent in Medical Devices. *Adv. Pharmacol. Sci.* **2012,** *2010*, 910686.
28. Klasen, H. J., Historical review of the use of silver in the treatment of burns. I. Early uses. *Burns* **2000,** *26* (2), 117.
29. Fox, C. L., Jr., Silver Sulfadiazine. A New Topical Therapy for Pseudomonas in Burns: Therapy of Pseudomonas Infection in Burns. *Arch. Surg.* **1968,** *96* (2), 184-188.
30. Melaiye, A.; Youngs, W. J., Silver and its application as an antimicrobial agent. *Expert Opin. Ther. Pat.* **2005,** *15* (2), 125-130.
31. Fox, C. L.; Modak, S. M., Mechanism of Silver Sulfadiazine Action on Burn Wound Infections. *Antimicrob. Agents Chemother.* **1974,** *5* (6), 582-588.
32. Zhang, S.; Du, C.; Wang, Z.; Han, X.; Zhang, K.; Liu, L., Reduced cytotoxicity of silver ions to mammalian cells at high concentration due to the formation of silver chloride. *Toxicol. in Vitro* **2013,** *27* (2), 739.
33. Pellei, M.; Gandin, V.; Marinelli, M.; Orsetti, A.; Del Bello, F.; Santini, C.; Marzano, C., Novel triazolium based 11th group NHCs: synthesis, characterization and cellular response mechanisms. *Dalton Trans.* **2015,** *44* (48), 21041.
34. Banti, C. N.; Giannoulis, A. D.; Kourkoumelis, N.; Owczarzak, A. M.; Poyraz, M.; Kubicki, M.; Charalabopoulos, K.; Hadjikakou, S. K., Mixed ligand-silver(I) complexes with anti-inflammatory agents which can bind to lipoxygenase and calf-thymus DNA, modulating their function and inducing apoptosis. *Metallomics* **2012,** *4* (6), 545-560.
35. Sanchez, O.; González, S.; Fernández, M.; Higuera-Padilla, A. R.; Leon, Y.; Coll, D.; Vidal, A.; Taylor, P.; Urdanibia, I.; Goite, M. C.; Castro, W., Novel silver(I) and gold(I)N-heterocyclic carbene complexes. Synthesis, characterization and evaluation of biological activity against tumor cells. *Inorg. Chim. Acta* **2015,** *437*, 143.
36. Allison, S. J.; Sadiq, M.; Baronou, E.; Cooper, P. A.; Dunnill, C.; Georgopoulos, N. T.; Latif, A.; Shepherd, S.; Shnyder, S. D.; Stratford, I. J.; Wheelhouse, R. T.; Willans, C. E.; Phillips, R. M., Preclinical anti-cancer activity and multiple mechanisms of action of a cationic silver complex bearing N-heterocyclic carbene ligands. *Cancer Lett.* **2017,** *403*, 98.
37. Eloy, L.; Jarrousse, A.-S.; Teyssot, M.-L.; Gautier, A.; Morel, L.; Jolivalt, C.; Cresteil, T.; Roland, S., Anticancer Activity of Silver-N-Heterocyclic Carbene Complexes: Caspase-Independent Induction of Apoptosis via Mitochondrial Apoptosis-Inducing Factor (AIF). *ChemMedChem* **2012,** *7* (5), 805-814.
38. Hartinger, C. G.; Dyson, P. J., Bioorganometallic chemistry from teaching paradigms to medicinal applications. *Chem. Soc. Rev* **2009,** *38* (2), 391.

39. R. Visbal; V. Fernández-Moreira; I. Marzo; A. Laguna; Gimeno, M. C., Cytotoxicity and biodistribution studies of luminescent Au(I) and Ag(I) N-heterocyclic carbenes. Searching for new biological targets.

. *Dalton Trans.* **2016,** *26*, 15026-15033.
40. Fourie, E.; Erasmus, E.; Swarts, J. C.; Tuchscherer, A.; Jakob, A.; Lang, H.; Joone, G. K.; Van Rensburg, C. E. J., Cytotoxicity of Hydrophylic Silver Carboxylato Complexes (vol 32, pg 519, 2012). *Anticancer Res.* **2012,** *32* (11), 5136-5136.
41. Liu, J. J.; Galettis, P.; Farr, A.; Maharaj, L.; Samarasinha, H.; McGechan, A. C.; Baguley, B. C.; Bowen, R. J.; Berners-Price, S. J.; McKeage, M. J., In vitro antitumour and hepatotoxicity profiles of Au(I) and Ag(I) bidentate pyridyl phosphine complexes and relationships to cellular uptake. *J. Inorg. Biochem.* **2008,** *102* (2), 303.
42. Santini, C.; Pellei, M.; Papini, G.; Morresi, B.; Galassi, R.; Ricci, S.; Tisato, F.; Porchia, M.; Rigobello, M. P.; Gandin, V.; Marzano, C., In vitro antitumour activity of water soluble Cu(I), Ag(I) and Au(I) complexes supported by hydrophilic alkyl phosphine ligands. *J. Inorg Biochem* **2011,** *105* (2), 232.
43. Abbehausen, C.; Heinrich, T. A.; Abrao, E. P.; Costa-Neto, C. M.; Lustri, W. R.; Formiga, A. L. B.; Corbi, P. P., Chemical, spectroscopic characterization, DFT studies and initial pharmacological assays of a silver(I) complex with N-acetyl-L-cysteine. *Polyhedron* **2011,** *30* (4), 579-583.
44. Cardoso, J. o. M. S.; Correia, I.; GalvÃ£o, A. M.; Marques, F.; Carvalho, M. F. N. N., Synthesis of Ag(I) camphor sulphonylimine complexes and assessment of their cytotoxic properties against cisplatin-resistant A2780cisR and A2780 cell lines. *J. Inorg. Biochem.* **2017,** *166*, 55.
45. L. Ortego; M. Meireles; C. Kasper; A. Laguna; M. D. Villacampa; Gimeno, M. C., Group 11 complexes with amino acid derivatives: Synthesis and antitumoral studies. *J. Inorg. Biochem.* **2016,** *156*, 133-144.
46. Zachariadis, Panagiotis C.; Hadjikakou, Sotiris K.; Hadjiliadis, N.; Skoulika, S.; Michaelides, A.; Balzarini, J.; De Clercq, E., Synthesis, Characterization and in Vitro Study of the Cytostatic and Antiviral Activity of New Polymeric Silver(I) Complexes with Ribbon Structures Derived from the Conjugated Heterocyclic Thioamide 2-Mercapto-3,4,5,6-tetra-hydropyrimidine. *Eur. J. Inorg. Chem.* **2004,** *2004* (7), 1420-1426.
47. Ciol, M. R.; Manzano, C. M.; Cuin, A.; Pavan, F. R.; Ribeiro, C. M.; Ruiz, A. L. T. G.; Oliveira, E. C. S.; Lustri, W. R.; Fregonezi, N. F.; Nogueira, F. A. R.; Corbi, P. P., A Silver Complex with Cycloserine: Synthesis, Spectroscopic Characterization, Crystal Structure and In Vitro Biological Studies. *ChemistrySelect* **2018,** *3* (6), 1719-1726.
48. D. Salvador-Gil; L. Ortego; R. P. Herrera; Marzo, I.; Gimeno, M. C., Highly active group 11 metal complexes with α-hydrazidophosphonate ligands. *Dalton Trans.* **2017,** *46*, 13745-13755.
49. Zaky, R. R.; Abdelghay, A. M., Synthesis, characterization and anticancerous properties of mixed ligand Pd(II) and Ag(I) complexes with 2-amino-7-oxo-4,5,6,7-tetrahydrobenzo[b]thiophene-3-carbonitrile and 2,2'-bipyridyl. *Res. J. Pharmaceut. Biol. Chem. Sci.* **2011,** *2*, 757-764.
50. Poyraz, M.; Banti, C. N.; Kourkoumelis, N.; Dokorou, V.; Manos, M. J.; SimÄiÄ, M.; GoliÄ-Grdadolnik, S.; Mavromoustakos, T.; Giannoulis, A. D.; Verginadis, I. I.; Charalabopoulos, K.; Hadjikakou, S. K., Synthesis, structural characterization and biological studies of novel mixed ligand Ag(I) complexes with triphenylphosphine and aspirin or salicylic acid. *Inorg. Chim. Acta* **2011,** *375* (1), 114.
51. Li, D.-D.; Fang, F.; Li, J.-R.; Du, Q.-R.; Sun, J.; Gong, H.-B.; Zhu, H.-L., Discovery of 6-substituted 4-anilinoquinazolines with dioxygenated rings as novel EGFR tyrosine kinase inhibitors. *Bioorg. Med. Chem. Lett.* **2012,** *22* (18), 5870-5875.

52. Zhang, D.; Yan, Y.; Jin, G.; Liu, B.; Ma, X.; Han, D.; Jia, X., Synthesis and antitumor evaluation of novel 4-anilino-7,8-dihydropyrido[4,3-d]pyrimidine-6(5H)-carboxylate derivatives as potential EGFR inhibitors. *Arch. Pharm.* **2018,** *351* (9), 1800110.
53. Mabkhot, Y. N.; Alatibi, F.; El-Sayed, N. N. E.; Al-Showiman, S.; Kheder, N. A.; Wadood, A.; Rauf, A.; Bawazeer, S.; Hadda, T. B., Antimicrobial Activity of Some Novel Armed Thiophene Derivatives and Petra/Osiris/Molinspiration (POM) Analyses. *Molecules* **2016,** *21*, 222.
54. Gramec, D.; Peterlin Mašič, L.; Sollner Dolenc, M., Bioactivation Potential of Thiophene-Containing Drugs. *Chem. Res. Toxicol.* **2014,** *27* (8), 1344-1358.
55. Lawrance, G. A., Coordinated trifluoromethanesulfonate and fluorosulfate. *Chem. Rev.* **1986,** *86* (1), 17-33.
56. van Geelen, C. M. M.; de Vries, E. G. E.; Le, T. K. P.; van Weeghel, R. P.; de Jong, S., Differential modulation of the TRAIL receptors and the CD95 receptor in colon carcinoma cell lines. *Br. J. Cancer* **2003,** *89* (2), 363-373.
57. Tolan, D.; Gandin, V.; Morrison, L.; El-Nahas, A.; Marzano, C.; Montagner, D.; Erxleben, A., Oxidative Stress Induced by Pt(IV) Pro-drugs Based on the Cisplatin Scaffold and Indole Carboxylic Acids in Axial Position. *Sci Rep* **2016,** *6*, 29367.
58. Marmol, I.; Castellnou, P.; Alvarez, R.; Gimeno, M. C.; Rodriguez-Yoldi, M. J.; Cerrada, E., Alkynyl Gold(I) complexes derived from 3-hydroxyflavones as multi-targeted drugs against colon cancer. *Eur. J. Med. Chem.* **2019,** *183*.
59. Marmol, I.; Virumbrales-Munoz, M.; Quero, J.; Sanchez-De-Diego, C.; Fernandez, L.; Ochoa, I.; Cerrada, E.; Yoldi, M. J. R., Alkynyl gold(I) complex triggers necroptosis via ROS generation in colorectal carcinoma cells. *J. Inorg. Biochem.* **2017,** *176*, 123-133.
60. Gonzalez-Barcia, L. M.; Fernandez-Farina, S.; Rodriguez-Silva, L.; Bermejo, M. R.; Gonzalez-Noya, A. M.; Pedrido, R., Comparative study of the antitumoral activity of phosphine-thiosemicarbazone gold(I) complexes obtained by different methodologies. *J. Inorg. Biochem.* **2020,** *203*.
61. Liu, X. H.; Rose, D. P., Differential expression and regulation of cyclooxygenase-1 and -2 in two human breast cancer cell lines. *Cancer Res.* **1996,** *56* (22), 5125-5127.
62. Sambuy, Y.; Angelis, I.; Ranaldi, G.; Scarino, M. L.; Stammati, A.; Zucco, F., The Caco-2 cell line as a model of the intestinal barrier: influence of cell and culture-related factors on Caco-2 cell functional characteristics. *Cell Biol. Toxicol.* **2005,** *21* (1), 1-26.
63. Badisa, R. B.; Darling-Reed, S. F.; Joseph, P.; Cooperwood, J. S.; Latinwo, L. M.; Goodman, C. B., Selective Cytotoxic Activities of Two Novel Synthetic Drugs on Human Breast Carcinoma MCF-7 Cells. *Anticancer Res.* **2009,** *29* (8), 2993-2996.
64. Xu, X. B.; Lai, Y. Y.; Hua, Z. C., Apoptosis and apoptotic body: disease message and therapeutic target potentials. *Bioscience Rep.* **2019,** *39*.
65. Saraste, A.; Pulkki, K., Morphologic and biochemical hallmarks of apoptosis. *Cardiovascular Res.* **2000,** *45* (3), 528-537.
66. Park, S. J.; Kim, I. S., The role of p38 MAPK activation in auranofin-induced apoptosis of human promyelocytic leukaemia HL-60 cells. *British J. Pharmacol.* **2005,** *146* (4), 506-513.
67. Park, N.; Chun, Y. J., Auranofin Promotes Mitochondrial Apoptosis by Inducing Annexin A5 Expression and Translocation in Human Prostate Cancer Cells. *J. Toxicol. Environ. Heal. - Part A Curr. Issues* **2014,** *77* (22-24), 1467-1476.
68. Redza-Dutordoir, M.; Averill-Bates, D. A., Activation of apoptosis signalling pathways by reactive oxygen species. *Biochim. Biophys. Acta - Mol. Cell Res.* **2016,** *1863* (12), 2977-2992.
69. Aubrey, B. J.; Kelly, G. L.; Janic, A.; Herold, M. J.; Strasser, A., How does p53 induce apoptosis and how does this relate to p53-mediated tumour suppression? *Cell Death Diff.* **2018,** *25* (1), 104-113.
70. Chen, J. D., The Cell-Cycle Arrest and Apoptotic Functions of p53 in Tumor Initiation and Progression. *Cold Spring Harb. Perspect. Med.* **2016,** *6* (3).
71. Moloney, J. N.; Cotter, T. G., ROS signalling in the biology of cancer. *Semin. Cell Dev. Biol.* **2018,** *80*, 50-64.

72. Ivanova, D.; Zhelev, Z.; Semkova, S.; Aoki, I.; Bakalova, R., Resveratrol Modulates the Redox-status and Cytotoxicity of Anticancer Drugs by Sensitizing Leukemic Lymphocytes and Protecting Normal Lymphocytes. *Anticancer Res.* **2019,** *39* (7), 3745-3755.
73. Eloy, L.; Jarrousse, A. S.; Teyssot, M. L.; Gautier, A.; Morel, L.; Jolivalt, C.; Cresteil, T.; Roland, S., Anticancer Activity of Silver-N-Heterocyclic Carbene Complexes: Caspase-Independent Induction of Apoptosis via Mitochondrial Apoptosis-Inducing Factor (AIF). *ChemMedChem* **2012,** *7* (5), 805-814.
74. Allison, S. J.; Sadiq, M.; Baronou, E.; Cooper, P. A.; Dunnill, C.; Georgopoulos, N. T.; Latif, A.; Shepherd, S.; Shnyder, S. D.; Stratford, I. J.; Wheelhouse, R. T.; Willans, C. E.; Phillips, R. M., Preclinical anti-cancer activity and multiple mechanisms of action of a cationic silver complex bearing N-heterocyclic carbene ligands. *Cancer Lett.* **2017,** *403*, 98-107.
75. Zhu, Z. L.; Du, S. S.; Du, Y. B.; Ren, J.; Ying, G. G.; Yan, Z., Glutathione reductase mediates drug resistance in glioblastoma cells by regulating redox homeostasis. *J. Neurochem.* **2018,** *144* (1), 93-104.
76. Quero, J.; Cabello, S.; Fuertes, T.; Marmol, I.; Laplaza, R.; Polo, V.; Gimeno, M. C.; Rodriguez-Yoldi, M. J.; Cerrada, E., Proteasome versus Thioredoxin Reductase Competition as Possible Biological Targets in Antitumor Mixed Thiolate-Dithiocarbamate Gold(III) Complexes. *Inorg. Chem.* **2018,** *57* (17), 10832-10845.
77. Zhang, X.; Frezza, M.; Milacic, V.; Ronconi, L.; Fan, Y. H.; Bi, C. F.; Fregona, D.; Dou, Q. P., Inhibition of Tumor Proteasome Activity by Gold-Dithiocarbamato Complexes via Both Redox-Dependent and -Independent Processes. *J. Cell. Biochem.* **2010,** *109* (1), 162.
78. Alva, N.; Panisello-Rosello, A.; Flores, M.; Rosello-Catafau, J.; Carbonell, T., Ubiquitin-proteasome system and oxidative stress in liver transplantation. *World J. Gastroenterol.* **2018,** *24* (31), 3521-3530.
79. Crespo, O.; Laguna, A.; Fischer, A., Structural characterization of silver(I) complexes [Ag(O3SCF3)(L)] (L=PPh3, PPh2Me, SC4H8) and [AgLn](CF3SO3) (n=2-4), (L=PPh3, PPh2Me). *Inorg. Chim. Acta* **2000,** *304*, 7-16.
80. Sanchez-de-Diego, C.; Marmol, I.; Perez, R.; Gascon, S.; Rodriguez-Yoldi, M. J.; Cerrada, E., The anticancer effect related to disturbances in redox balance on Caco-2 cells caused by an alkynyl gold(I) complex. *J. Inorg. Biochem.* **2017,** *166*, 108-121.